Applied Thermal Engineering 31 (2011) 3463–3478

Contents lists available at ScienceDirect

Applied Thermal Engineering

journal homepage: www.elsevier.com/locate/apthermeng

Modeling of fire-tube boilers

F.J. Gutiérrez Ortiz*

Departamento de Ingeniería Química y Ambiental, Universidad de Sevilla, Camino de los Descubrimientos s/n, 41092 Sevilla, Spain

ARTICLE INFO

Article history:
Received 21 December 2010
Accepted 2 July 2011
Available online 13 July 2011

Keywords:
Fire-tube boiler
Modeling
Simulation
Heat transfer
Steam
Fuel

ABSTRACT

In fire-tube boilers, the flue gas passes inside boiler tubes, and heat is transferred to water on the shell side. A dynamic model has been developed for the analysis of boiler performance, and Matlab has been applied for integrating it. The mathematical model developed is based on the first principles of mass, energy and momentum conservations. In the model, the two parts of the boiler (fire/gas and water/steam sides), the economizer, the superheater and the heat recovery are considered. The model developed can capture the dynamics of the boiler level and boiler pressure with confidence, and it is adequate to approach the boiler performance and, hence, to design and test a control strategy for such boilers. Furthermore, it gives insight of dynamics performance not only during nominal operating conditions, or transient behavior when a parameter is changed, but also for the start-up. The model proposed can be easily implemented and thus, it is useful to assist plant engineers and even for training future operators. A case study of an 800 HP fire-tube boiler burning fuel-oil has been simulated to test the boiler performance by varying operating conditions using a pulse and a step change in fuel and steam flow-rate as well as simulating a start-up form the beginning up to achieve the steady state. The results match qualitatively well when compared to results from the literature.

1. Introduction

The design of fire-tube boilers consists of a bundle of fire tubes contained in a shell and the evaporating process takes place outside the fire tubes generating steam. Fire-tube boilers are often characterized by their number of passes, referring to the number of times that the flue gas flows along the length of the pressure vessel transferring heat to the water. Each pass sends the flue gas through the tubes in the opposite direction. To make another pass, the gas turns 180° and passes back through the shell. The turnaround zones can be either dry-back or water-back. In dry-back designs, the turnaround area is refractory lined. In water-back designs, this turnaround zone is water-cooled, eliminating the need for the refractory lining. Their characteristically large water capacity makes them somewhat slow in coming up to operating pressure and temperature but, on the other hand, the large amount of heat stored in the water provides some accumulator action that makes it possible to meet load changes quickly.

There are several fire-tube boiler designs such as the horizontal return tubular boiler (HRT), which is encased in a brickwork setting to contain the flame, so it was an externally fired boiler and also two-pass boiler. By enlarging the diameter of the return flue and putting the firing grating inside this enlarged flue the HRT boiler becomes internally-fired and the furnace is placed inside the shell and completely surrounded by water. By this way, the boiler has a large heating surface and a reasonably long gas travel, and does not require external brickwork. Thus, by eliminating the external brickwork the design converts into a Scotch Marine boiler since it was extensively used for marine service. Now, the hot gases flow from the fire to the reversing chamber at the rear of the boiler and then forward again through the fire tubes. All parts are inside the shell and completely surrounded by water. In earlier days, the basic fire-tube boiler was manufactured at the factory, and the refractory, insulation, boiler fittings, controls and firing equipment were installed by others. The modern fire-tube boiler is marketed as a packaged unit, and now the majority of fire-tube boilers are packaged type fire-tube boiler. The boiler as supplied by the manufacturer comes as a completely equipped unit mounted on its own base, ready for operation as soon as it is placed in the boiler room and hooked up to the various supply and discharge piping. The diagrams in Fig. 1 show the basic gas-flow patterns used today. All use an internal furnace or firebox as a first pass, then route the gases into various tube layouts. Fig. 2 shows a schematic representation of a typical three-pass fire-tube boiler.

Another type of fire-tube boiler is the vertical fire-tube boiler, which is similar in construction to the horizontal fire-tube boiler. It is

* Tel.: +34 95 448 72 68; fax: +34 95 446 17 75.
E-mail address: fjgo@esi.us.es.

1359-4311/$ – see front matter © 2011 Elsevier Ltd. All rights reserved.
doi:10.1016/j.applthermaleng.2011.07.001

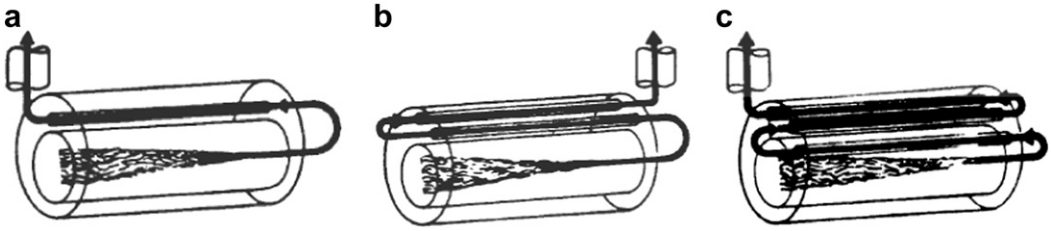

Fig. 1. Basic gas flow patterns of a fire-tube (a) two-pass; (b) three-pass; (c) four-pass.

basically made of a round steel drum or shell. Both ends of the shell are closed by flat plates called tube sheets. The combustion of the fuel takes place in a furnace and the hot gases travel from the furnace through the fire tubes to the chimney. The water in the boiler shell surrounds the fire tubes. The gases travel through the boiler in one direction only and for this reason, this boiler can also be classed as a single-pass boiler. Vertical fire-tube boilers have an advantage when floor space is limited as they occupy only a small area.

Some recent papers have been published regarding with other aspects of fire-tube boilers [1,2]. Thus, effects of the addition of solid surface on carbon monoxide (CO) emission reduction have been investigated in a combustion chamber of a three-pass fire tube water heater [1] and optimization of fire tube heat recovery steam generators through genetic algorithm has been carried out by moving variables toward reducing the operational costs of the HRSG, reducing thus the heat loss.

Dynamic modeling and simulation are becoming increasingly important in engineering to analyze the unsteady operation of complex systems [3]. Several studies of modeling the boiler evaporation system can be found in the literature, especially for water-tube boilers [4–7], but barely for fire-tube boilers. In this work, the modeling of the heat transfer between flue gas and water in a fire-tube boiler is considered. In the literature, a comprehensive modeling for fire-tube boilers has not been treated. Generally, the few models found are focused to one aspect of the fire-tube boiler performance as the gas/fire side or the water/steam side, and normally centered on nominal operating conditions. However, a simulator must include the gas/fire side and the water/steam side performance as well as both the nominal operation and the start-up/shut-down of the fire-tube boiler.

CFD models are a powerful tool to model very complicated systems such as for instance turbulent diffusion flames. CFD predicts flow, mixing, combustion, heat release and heat transfer. There are some modeling works carried out using CFD code [8–12]. However, these models are highly dependent on initial and boundary conditions as well as the arrangement of grid nodes and turbulence model. Therefore, the results are only good as the input data, and there are still limitations in the physical models in the codes. Thus, for instance, the empirical k-ϵ model has been used for many years and has been widely used despite its many known limitations. Indeed, in turbulence models the magnitudes of two turbulence quantities, the turbulence kinetic energy k and its dissipation rate ϵ, are calculated from transport equations solved simultaneously with those governing the mean flow behavior. Thus, new modeling papers continuously present methods in order to overcome the assumptions and simplifications followed in boiler modeling by preceding models. The reliability of CFD analysis depends heavily on the turbulence model employed together with the wall functions implemented. In order to resolve the abrupt fluctuations experienced by the turbulent energy and other parameters (many times selected in a heuristic way, conferring to the modeling a semi-empirical characteristic) located at near wall regions and shear layers a particularly fine computational mesh is necessary which inevitably increases the computer storage and run-time requirements. Moreover the dynamic response is very complex to address by CFD modeling. Thus, the assessment of a fire-tube boiler may be simplified by a model such as that described in this paper, for practical purposes.

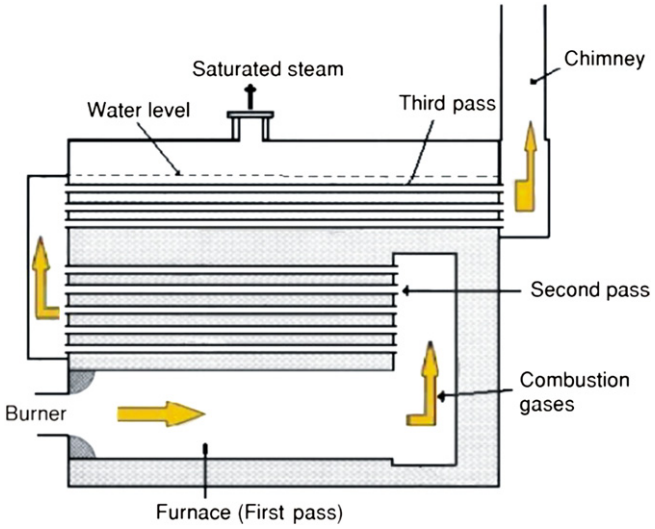

Fig. 2. Schematic representation of a typical three-pass fire-tube boiler [29].

In this work, the aim is to propose a model for simulating the performance of a horizontal packaged fire-tube boiler in a realistic way, although with simplifications. A simulation tool may be useful to approach the dynamic performance of a boiler in order to assist the plant engineer and even to train the technical staff. Furthermore, a simplified model is better in practice if a control system must be included. Detailed modeling of plants dynamics is not normally efficient for control purposes, since the plant model should describe the plant dynamics with sufficient accuracy and not describe the microscopic details occurring within individual plant components [13]. However, in order to better understand the final model used to simulate the fire-tube boiler performance, first it is convenient to establish a more rigorous model in order to recognize the simplifications made after.

By means of simulations the plant engineer and operators can evaluate changes in operating conditions and select in real-time the best way to operate the furnace and evaporation system. Thus, simulation is useful both for training and assisting in making on-line decisions. One of the aims of the dynamic model developed is to achieve reliable predictions on the changes of the more relevant variables so it could be used, e.g., for the design of the unit control.

2. Outline of the model

Description of the dynamic performance of a distributed parameters thermal system like a fire-tube boiler needs to solve a set of partial differential equations. Furthermore, some additional

algebraic equations are required leading to an overall DAE mathematical system that is very complex to solve. Additionally, some non-linearities arise when modeling heat transfer mechanism such as radiation or even convection coupled with empirical correlations. Temperature, pressure and flow-rate of participating fluids are normally the independent variables. Besides, some restrictions and interlocks should be taken into account to operate the boiler in a safe way. Therefore, the real problem is very difficult to solve even numerically. Hence, a comprehensive model is proposed and after simplified to reduce the complexity and the computational time, but providing reasonable results.

The model is based on the mass, energy and momentum balances together with constitutional equations. Two parts are distinguished in fire-tube boilers: the fire/gas side, integrated by the combustion chamber as well as by the successive gas passes (through the tube banks), and the water/steam side, which contents liquid water evaporating in the lower zone and saturated vapor or steam in the upper zone, from which it is continuously withdrawing to the points of use through a control valve.

In order to evaluate the energy usage of the boiler, the reaction chamber has been divided in different zones (slices) as shown in Fig. 3, with all the fuel and the air being fed into the first zone. The reaction chamber is modeled as a series of continuous stirred tank reactors, and the main reactions that take place into the chamber occur in a very fast way. The wall tubes have been also discretized into slices in the direction of gas flow to facilitate the calculations of the heat transfer. Fig. 4 shows the heat transfer phenomena that occur in the boiler: transfer by radiation and convection between the combustion gases and wall tubes, conduction through wall tubes to water, transfer by convection from tubes to liquid–water vapor mixture in the different passes. The gas phase is considered an ideal gas, and the conduction in this phase is neglected. Heat transfer from the gas to the combustion chamber wall is calculated by both radiation and convection. The axial component of radiation can be reasonably neglected since it is relatively small compared to the radial component. All quantities are the same in a cross section of the tube, i.e., no fluid pressure and temperature gradients occur in the radial and circumferential directions. Finally, since hydrodynamics changes are much faster than thermal or gas composition changes, the hydrodynamics will be solved as a steady state problem.

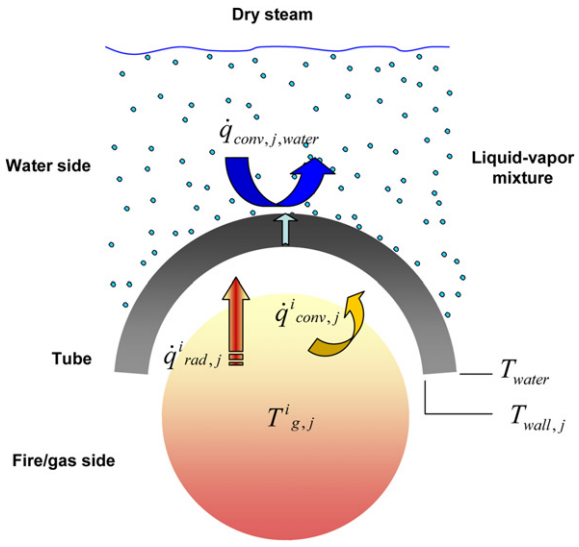

Fig. 4. Schematic heat transfer phenomena occurring within a fire-tube boiler (under the water or phase-).

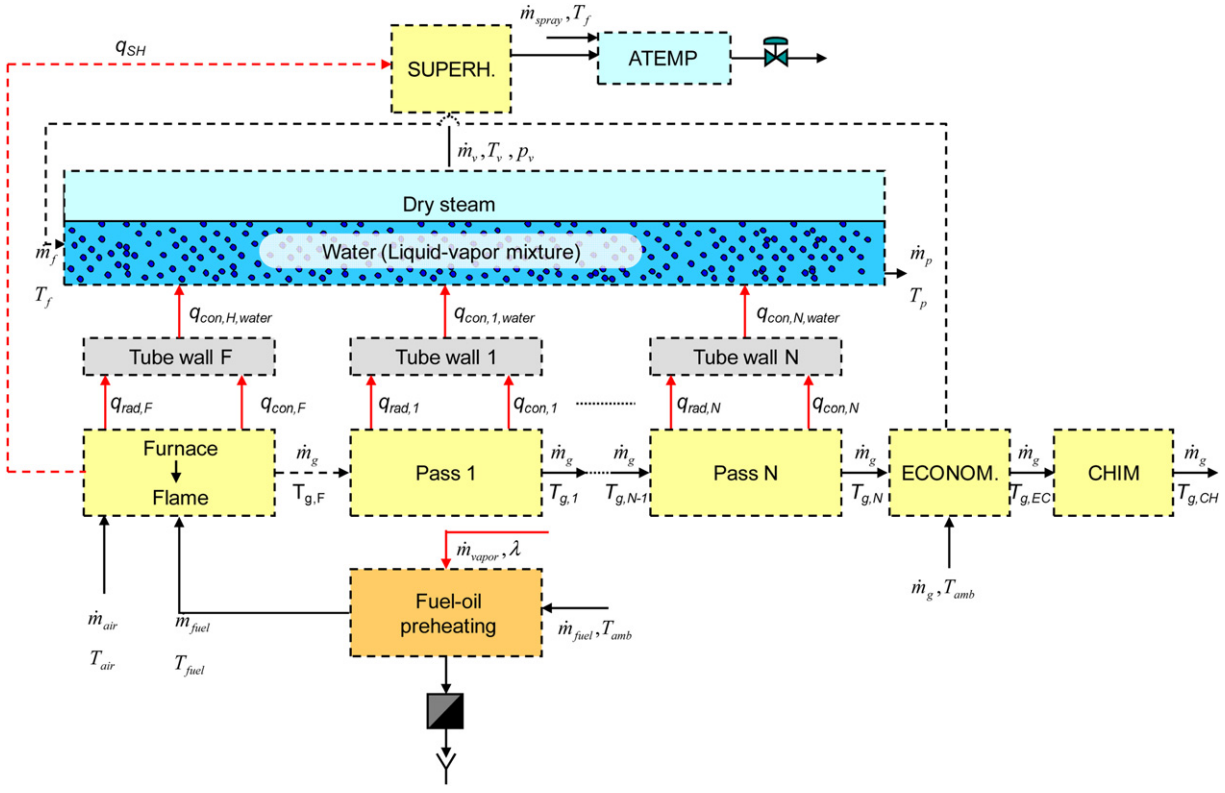

Fig. 3. Scheme for the modeling of a fire-tube boiler.

3. Model development

To build a model for a system by physical principles, it is necessary to define inputs and outputs. For a fire-tube boiler, the inputs are design parameters (boiler geometry and elements optionally incorporated as an economizer, a superheater or a degasifier) and operational parameters, such as the feed water, fuel and air flow-rates and the steam valve position), fuel and ambient temperature and pressure.

The outputs are performance parameters such as temperatures (boiler water, flue gas, saturated and superheated steam), pressures (inside water phase boiler and steam phase boiler), steam flow-rate, level or liquid volume, composition of flue gas and global boiler efficiency. Moreover, there may be other outputs depending on the complementary elements disposed as heat recovery by flashing of blowdown, degasifier, heat exchanger, conditioning of the steam through a superheater or the feed water by an economizer. These other parts of the fire-tube boiler are after taken into account. Next, the modeling will be focused on the aforementioned two parts of the fire-tube boiler.

3.1. Fire/gas side

It is assumed that combustion is controlled by the mixing rate and thus all mixed is burnt. Hence, combustion reactions are assumed to be very fast and shifted to the products side in the reaction equations, due to the temperature conditions inside the combustion chamber. Therefore, reactions kinetics are ignored by proposing that reactions are instantaneous and proceed wherever gas and air coexist, to give a mixture of combustion products plus some residual reactants. In this way, it can be avoided the enormous computational task required in the modeling of many interconnected chemical reactions involved in the combustion of a fuel.

The fuel consumption is assumed to be constant in a nominal operation, but it is variable once the system is under control. The air–fuel ratio is assumed to be constant, in a nominal operation, but it is variable once the system is under control, where the oxygen concentration in the flue gas can be set by the plant engineer. Heating value and moisture content of the fuel are constant.

Heat transmission inside the combustion chamber takes place between a mixture of moving gases and the tube walls. The calculation of this heat transfer requires to know the gas composition, physical properties of the gas and temperature in both the combustion chamber and walls. The furnace or combustion chamber is assumed to be filled of a gray emitting, absorbing, and isotropically scattering medium and surrounded by gray walls. Turbulent heat transfer is assumed throughout the process.

For the wall of furnace, a representative temperature is used as well as for the other tubes of the gas passes. The assumption of uniform surface temperature is reasonable for predicting heat transfer within the combustion chamber when compared with experimental results with detailed mathematical models of the furnace [14]. Since the wall temperature will be quite lower than the gas temperature, the radiation from the wall to the combustion products is very much less that in the opposite direction.

As aforementioned, and according to the one-dimensional assumptions in the modeling, the combustion chamber (first pass of gas) is discretized in N_F slices. Thus, for all the components, k, in each slice, i:

$$\frac{\mathrm{d}}{\mathrm{d}t}m_k^i = \dot{m}_{k,in}^i - \dot{m}_{k,out}^i - \dot{m}_{k,cons}^i + \dot{m}_{k,gen}^i = \dot{m}_k^{i-1} - \dot{m}_k^i - \dot{m}_{k,cons}^i + \dot{m}_{k,gen}^i = 0 \quad (1)$$

$$\dot{m}_{fuel} + \dot{m}_{air} = \dot{m}_g;\ V_g = V_F = V \quad (2)$$

The heat flux can be captured by using the lower heating value (LHV) of the fuel as follows:$\dot{m}_{\mathrm{fuel}}LHV$ (chemical energy of fuel).

Likewise, the variation of the fractional heat release due to combustion (Y) with axial distance (or slice, in this case) from the jet orifice may be described by an exponential expression where the constant 4.6 means that 99% of the heat release occurs at the end of the flame (at the end of the furnace), as follows:

$$Y = 1 - \exp\left(-4.6\frac{x}{L_F}\right) \quad (3)$$

From hence, the fractional heat release within zone or slice, i, results in the following:

$$\Delta Y_i = Y_i - Y_{i-1} = \exp\left(-4.6\frac{i-1}{N_F}\right) - \exp\left(-4.6\frac{i}{N_F}\right) \quad (4)$$

For the average convective film coefficient, it has been used the classical Dittus–Boelter heat transfer correlation for fluids in turbulent flow. Likewise, the equation for the radiation heat flow follows the suggestion of Hottel and Sarofim [15] under the assumption of gray gases and gray wall. Since all participating surfaces behave as gray-Lambert surfaces are assumed in the model, total emissivity and total absorptivity are equal. This consideration simplifies the analysis of radiation transfer and it does not lead to significant predictive error.

Thus, in each slice i of the furnace:

$$\frac{\mathrm{d}}{\mathrm{d}t}\left(\rho_{g,H}VC_{v,g,F}T_{g,F}^i\right) = \dot{m}_{\mathrm{fuel}}LHV\left[\exp\left(-4.6\frac{i-1}{N_F}\right) - \exp\left(-4.6\frac{i}{N_F}\right)\right] + \dot{m}_g\overline{C}_{p,g,F}\left(T_{g,F}^{i-1} - T_{g,F}^i\right) - \dot{q}_{\mathrm{rad},F}^i - \dot{q}_{\mathrm{conv},F}^i \quad (5)$$

where

$$\dot{q}_{\mathrm{conv,F}}^{\mathrm{i}} = \overline{h}_{c,F}\frac{2\pi R_{\mathrm{int},F}L_F}{N_F}\left(T_{g,F}^i - T_{\mathrm{wall},F}\right);$$

$$\overline{h}_{c,F} = 0.023\frac{k_{g,F}}{2R_{\mathrm{int},F}}\mathrm{Re}^{0.8}\mathrm{Pr}^{0.4};\ \overline{T}_{g,F} = \sum_{i=1}^{N_F}\frac{T_{g,F}^i}{N_F} \quad (6)$$

$$\dot{q}_{\mathrm{rad},F}^i = \frac{2\pi R_{\mathrm{int},F}L_F}{N_F}\sigma\frac{\varepsilon_{\mathrm{wall},F}\varepsilon_{g,F}}{\varepsilon_{g,F} + \varepsilon_{\mathrm{wall},F} - \varepsilon_{\mathrm{wall},F}\varepsilon_{g,F}}\left(T_{g,F}^{i\,4} - T_{\mathrm{wall},F}^{\ 4}\right) \approx \frac{2\pi R_{\mathrm{int},F}L_F}{N_F}\sigma\frac{\varepsilon_{\mathrm{wall},F}+1}{2}\varepsilon_{g,F}\left(T_{g,F}^{i\,4} - T_{\mathrm{wall},F}^{\ 4}\right) \quad (7)$$

Through a good burner design and control, the occurrence of soot in the flame is usually avoided. Hence, the combustion from luminous radiation from these flames is small and it could be disregarded. Furthermore, with a very poor mixing, some luminosity may be produced, although this possibility is ignored since a good mixing is assumed. Nevertheless, the model proposed may include the luminous radiation that is usually important with liquid and solid fuels, although it is normally not significant for gaseous fuel. The soot emissivity may be represented by a single gray gas expression because the soot radiation continuous across the wavelength spectrum. The soot generated in a flame is highly dependent, among other things, on the fuel composition. Talmor [16] correlated the flame emissivity with the fuel type. For fuel

gases with C/H weight ratio between 3.5 and 5.0 the data were correlated by either of two correlations:

$$\varepsilon = 0.20\sqrt{\frac{LHV}{900}} \tag{8}$$

where LHV is the lower heating value of the fuel in Btu/ft^3, or

$$\varepsilon = 0.048\sqrt{MW_{\text{fuel}}} \tag{9}$$

where MW_{fuel} is the molecular weight of the fuel.

For liquid fuels with C/H weight ratios between 5 and 15, the following correlation was determined:

$$\varepsilon = 1 - 68.2\exp\left(-2.1\sqrt{C/H}\right) \tag{10}$$

where C/H is the weight ratio of carbon to hydrogen for the fuel.

Thus, the emissivity related to flames of hydrogen, natural gas, gas oil and residual fuel-oil are 0.17, 0.21, 0.61 and 0.85, respectively. This simplified approach allows to avoid the addition of more coefficients to calculate a weighted overall emissivity of flame, in case of accounting for any kind of flame related to a given fuel.

For the other gas passes (second and so on) through a given tube bank, j ($j = 2$, 3 and 4), a number of tubes, $n_{t,j}$, has to be considered:

$$\frac{1}{n_{t,j}}\frac{\mathrm{d}}{\mathrm{d}t}\left(V_j C_{v,g,j}\rho_{g,j}T^i_{g,j}\right) = \frac{\dot{m}_g}{n_{t,j}}\overline{C}_{p,g}\left(T^{i-1}_g - T^i_g\right) - \dot{q}^i_{conv,j} \tag{11}$$

Each tube of any pass (from the second pass of gas) may be also discretized in N_j slices

$$\dot{q}^i_{\text{conv},j} = \overline{h}_{c,j}\frac{2\pi R_{\text{int},j}L_j}{N_j}\left(T^i_{g,j} - T_{wall,j}\right);$$

$$\overline{h}_{c,j} = 0.023\frac{k_{g,j}}{2R_{\text{int},j}}\text{Re}^{0.8}\text{Pr}^{0.4};\ \overline{T}_{g,j} = \sum_{i=1}^{N_j}\frac{T^i_{g,j}}{N_j} \tag{12}$$

$$\dot{q}^i_{\text{rad},j} = \frac{2\pi R_{\text{int},j}L_j}{N_j}\sigma\frac{\varepsilon_{wall,j}+1}{2}\varepsilon_{g,j}\left(T^i_{g,j}4 - T^4_{wall,j}\right) \tag{13}$$

The momentum balance for all the fire/gas side:

$$\left[\frac{P_{in,g,j}}{\rho_{g,j}g} + z_{in} + \frac{v_{in,g,j}{}^2}{2g}\right] - \left[\frac{P_{out,g,j}}{\rho_{g,j}g} + z_{\text{out}} + \frac{v_{out,g,j}{}^2}{2g}\right] = h_{fr,j} \tag{14}$$

$$\sum_{\forall j} h_{fr,j} = \left(H_{burner} + H_{fan}\right) \tag{15}$$

Equation (11) represents the mechanical energy loss expressed in meters of w.c. and Equation (12) represents the energy to be supplied by the burner blower and the flue-gas fan.

Regarding with the metal section, the equations for the combustion chamber (first pass for gases) are the following:

$$m_{t,F}C_{p,t_F}\frac{\mathrm{d}}{\mathrm{d}t}T_{wall,F} = \left(\sum_{i=1}^{N_F}\left(\dot{q}^i_{rad,F} + \dot{q}^i_{conv,F}\right) - \dot{q}_{F,water}\right) \tag{16}$$

where

$$\dot{q}_{F,water} = \frac{2\pi R_{ext,F}L_F}{\frac{R_{\text{ext},F}}{k_{t,F}}\ln\left(\frac{R_{ext,F}}{R_{\text{int},F}}\right) + \frac{1}{\overline{h}_{c,water}}}\left(T_{wall,F} - T_{water}\right) \tag{17}$$

Similarly, for the j-th gas pass:

$$m_{t,j}C_{p,t_j}\frac{\mathrm{d}}{\mathrm{d}t}T_{wall,j} = \left(n_{t,j}\sum_{i=1}^{N_j}\left(\dot{q}^i_{rad,j} + \dot{q}^i_{conv,j}\right) - \dot{q}_{j,water}\right) \tag{18}$$

$$\dot{q}_{j,water} = \frac{2\pi n_{t,j}R_{ext,j}L_j}{\frac{R_{\text{ext},j}}{k_{t,j}}\ln\left(\frac{R_{ext,j}}{R_{\text{int},j}}\right) + \frac{1}{\overline{h}_{c,water}}}\left(T_{wall,j} - T_{water}\right) \tag{19}$$

3.2. Water/steam side

Fig. 5 shows a scheme of a cross section of the boiler for the water/steam side. It has one incoming stream, the feed water ($\dot{m}_f$). There are two outgoing streams: the drain/purge water or blow-down ($\dot{m}_p$) and the produced steam leaving the shell ($\dot{m}_v$). The shell space is separated into two zones by the surface of water. The zone above this surface is called the upper/steam zone. The other is called the lower/liquid zone. Hence, the mass balance equations are written following the above hypotheses and the scheme shown in Fig. 5. Feed water temperature is assumed to be constant in a nominal operation, but it is variable once the system is under control.

In the water side or boiler shell side, water is exposed to the heated surface of tubes. Around this zone, the temperature is higher and, hence, with a lower density than the rest of surrounding water. The density differences promote the natural circulation of water elements that are heated and are lighter, conveying thus, by this way, the heat flux to the surroundings. Therefore, water moves up and reaches the water surface and there evaporates. The boiling two-phase mixture flows on the shell side, across the horizontal submerged tube bundle, while the heating fluid flows inside the tubes. The natural circulation is governed by the density differences between the mixture within the shell (lower void fraction and higher density) and the boiling two-phase mixture in the bundle arrangement (higher void and lower density). Although, the rigorous development of the boiling (pool boiling that considers consider the two phases clearly defined under water) is outside the scope of the paper, in order to account for the effective heat transfer due to boiling (much

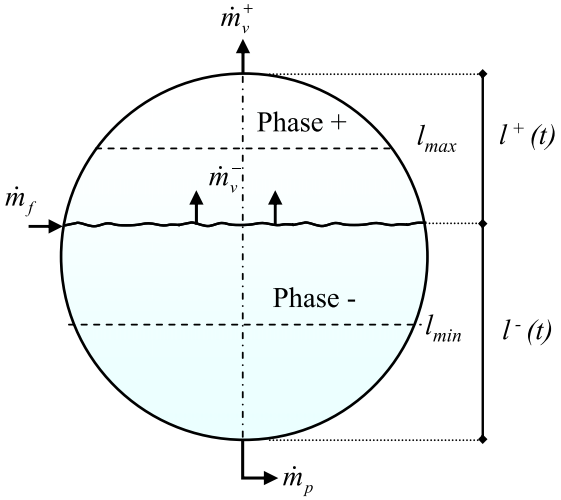

Fig. 5. Cross section view of a fire-tube boiler. Water/steam side (the fire–tubes are not shown).

larger than those for simple natural convection to the liquid), the Cooper pool boiling correlation [17] may be used for calculating the nucleate pool boiling heat transfer coefficient, although the model does not consider the two phases clearly defined under water. By taking a surface roughness of the boiling surface of 1 μm, and applying to water, it results the following correlation to be used:

$$h_{nb} = 12.96 p_r^{0.12}(-0.4343\ln p_r)^{-0.55}(Q/A)^{0.67} \quad (20)$$

The heat flux (Q/A) is in W/m^2. For a range of pressures from 2 to 15 bar, and using fuel-oil with the nominal fuel flow-rate, h ranges from 4260 to 7419 W/m^{2}K.

Initially, the model considers that liquid–vapor mixture in the overall system is not in equilibrium, so the system pressure is not uniform and equal to the saturation pressure corresponding to the mixture temperature. Thus, two pressure values (similar but not equal) are taken into account.

The presence of steam bubbles below the liquid level in the drum may cause the water level rapidly shrinks or swells due to collapse or expansion of steam bubbles below the water level when, for instance, a sudden change in the steam flow-rate occurs. This leads to a change in the level in the sense intuitively reverse to what one would expect through the transient size in the steam bubbles. Many modeling effort has been addressed to describe the shrinks-swell phenomenon, due to the mechanics of the natural convection circulation of water within the steam generator in water-tube boilers. However, in fire-tube boilers, with a relatively large chamber shell, it may be assumed a complete separation of steam and water inside the shell, and predict the water level reasonably if only a small amount of steam exists below the water level because, in opposition to water-tube boilers, the steam bubbles do not come from a riser where the rising rate of steam in water (calculated from the drift-flux type equation) determines actual flow-rate of steam under the water crossing the water surface to the steam phase. Indeed, the drum behavior in water-tube boilers when the steam valve is suddenly opened responds to a transient due the flow-rate of the two-phase flow in the riser, as a consequence of the large/small amount of boil-up from most of the tubes in the boiler. Thus, for a fire-tube boiler model, it is not required to account for a condensation model of steam in water under the water surface. Consequently, liquid temperature may be considered to be equal to the saturation temperature corresponding to the shell pressure (initially, that in the liquid zone); that is, instantaneous evaporation takes place in the liquid side when the shell pressure changes.

- Vapor phase (dry steam) in the upper zone (phase +)

$$\text{Mass balance}: \frac{\mathrm{d}}{\mathrm{d}t}m^+ = \frac{\mathrm{d}}{\mathrm{d}t}\left(\rho^+V^+\right) = \rho^+\frac{\mathrm{d}}{\mathrm{d}t}V^+ + V^+\frac{\mathrm{d}}{\mathrm{d}t}\rho^+ = \dot{m}_v^- - \dot{m}_v^+ \quad (21)$$

$$V^+ = A_l^+ L \cong \left[\frac{\pi}{2}R^2 - \frac{R^3 + R^2 l^+ - 3Rl^{+2} + l^{+3}}{\sqrt{2Rl^+ - l^{+2}}}\right]L = f_0^+\left(l^+\right) \quad (22)$$

$$\frac{\mathrm{d}V^+}{\mathrm{d}t} = \frac{\mathrm{d}V^+}{\mathrm{d}l^+}\frac{\mathrm{d}l^+}{\mathrm{d}t} = f_1^+\left(l^+\right)\frac{\mathrm{d}l^+}{\mathrm{d}t};\ f_1^+\left(l^+\right) = \frac{\mathrm{d}f_0^+\left(l^+\right)}{\mathrm{d}t} \quad (23)$$

$$f_1^+\left(l^+\right) = -\frac{L}{2Rl^+ - l^{+2}}\begin{bmatrix}\left(R^2 - 6Rl^+ + 3l^{+2}\right)\sqrt{2Rl^+ - l^{+2}} \\ -\left(R^3 + R^2 l^+ - 3Rl^{+2} + l^{+3}\right)\dfrac{2\left(R - l^+\right)}{\sqrt{2Rl^+ - l^{+2}}}\end{bmatrix} \quad (24)$$

$$\text{Energy balance}: \frac{\mathrm{d}}{\mathrm{d}t}\left(\rho^+V^+u^+\right) = \rho^+V^+\frac{\mathrm{d}}{\mathrm{d}t}u^+ + u^+\frac{\mathrm{d}}{\mathrm{d}t}\left(\rho^+V^+\right) = \dot{m}_v^- h^- - \dot{m}_v^+ h^+ \quad (25)$$

By considering the steam mass flow-rate crossing the water surface as a function of the pressures difference between phases and a control valve for the steam leaving the boiler:

$$\frac{\mathrm{d}}{\mathrm{d}t}\left(\rho^+V^+\right) = \rho^+ f_1^+\left(l^+\right)\frac{\mathrm{d}}{\mathrm{d}t}l^+ + f_0^+\left(l^+\right)\frac{\mathrm{d}}{\mathrm{d}t}\rho^+ = \dot{m}_v^- - \dot{m}_v^+ = K^-\left(P^- - P^+\right) - K_{VS}C^s f(x)\sqrt{\left(P^+ - P_{\mathrm{sum}}\right)\rho^+} \quad (26)$$

where C^s and $f^s(x)$ are a conversion factor of units and the inherent characteristic for the steam control valve, respectively. From Equations (25) and (26), it results:

$$m^+\frac{\mathrm{d}u^+}{\mathrm{d}t} = \dot{m}_v^- h^- - \dot{m}_v^+ h^+ - \dot{m}_v^- u^+ + \dot{m}_v^+ u^+ \quad (27)$$

$$\frac{\mathrm{d}}{\mathrm{d}t}T^+ = \frac{1}{m^+\overline{C}_v^+}\begin{bmatrix}\dot{m}_v^-\left(\overline{C}_p^- T^- + \lambda^- - \overline{C}_v^+ T^+ - \lambda^+\right) - \\ K_{VS}C^s f^s(x)\sqrt{\left(P^+ - P_{sum}\right)\rho^+}\begin{pmatrix}\left(\overline{C}_p^+ T^+ + \lambda^+\right) \\ -\left(\overline{C}_v^+ T^+ + \lambda^+\right)\end{pmatrix}\end{bmatrix}$$

$$= \frac{1}{m^+\overline{C}_v^+}\left[\dot{m}_v^-\left(\overline{C}_p^- T^- - \overline{C}_v^+ T^+\right) - K_{VS}C^s f^s(x)P^+\sqrt{\frac{\left(P^+ - P_{\mathrm{sum}}\right)}{\rho^+}}\right] \quad (28)$$

where it has been made an approach for the last term as $T^+(\overline{C}_p - \overline{C}_v) \cong P^+/\rho^+$. As $\lambda^+ \approx \lambda^-$:

$$\frac{\mathrm{d}}{\mathrm{d}t}T^+ = \frac{1}{\rho^+ f_0^+\left(l^+\right)\overline{C}_v^+}\left[K^-\left(P^- - P^+\right)\left(\overline{C}_p^- T^- - \overline{C}_v^+ T^+\right) - K_{VS}C^s f^s(x)P^+\sqrt{\frac{\left(P^+ - P_{\mathrm{sum}}\right)}{\rho^+}}\right] \quad (29)$$

- Liquid phase (water) in the lower zone (phase −)

$$\frac{\mathrm{d}}{\mathrm{d}t}\left(\rho^-V^-\right) = \rho^-\frac{\mathrm{d}}{\mathrm{d}t}V^- + V^-\frac{\mathrm{d}}{\mathrm{d}t}\rho^- = \dot{m}_f - \dot{m}_p - \dot{m}_v^-,\quad P^- = P^-\left(T^-\right) \quad (30)$$

$$\frac{\mathrm{d}}{\mathrm{d}t}T^- = \frac{1}{\rho^-\left(V_{total} - f_0^+\left(l^+\right)\right)\overline{C}_v^-}\begin{bmatrix}\dot{m}_f\left(h_{p,f}\left(T_f\right) - u^-\left(T^-\right)\right) - \dot{m}_p\left(h_l^-\left(T^-\right) - u^-\left(T^-\right)\right) - \\ -K^-\left(P^- - P^+\right)\left(h_v^-\left(T^-\right) - u^-\left(T^-\right)\right) + \sum_{j=1}^{2,3,4}\dot{q}_{j,water}\end{bmatrix} \quad (31)$$

$$x_v^- = \frac{m_v^-}{m^-} = const.\ (data) \tag{32}$$

$$\rho^- = \frac{1}{v^-};\ v^- = \left(1 - x_v^-\right)v_l^- + x_v^- v_v^- \tag{33}$$

$$h^- = \left(1 - x_v^-\right)h_l^- + x_v^- h_v^-;\ h_l^- = h_l^-\left(T^-\right);\ h_v^- = h_v^-\left(T^-\right) \tag{34}$$

$$u^- = \left(1 - x_v^-\right)u_l^- + x_v^- u_v^-;\ u_l^- = u_l^-\left(T^-\right);\ u_v^- = u_v^-\left(T^-\right) \tag{35}$$

4. Simplified model

The solution of the model equations is very difficult due to non-linearities and the DAE nature of the model. Thus, the model will be simplified to numerically solve it, including the boiler start-up, without consuming a long time. Once started the boiler and achieved the nominal operating conditions (steady state), the process must be kept under control in order to provide the demanded vapor at the set pressure. The static model (without storage terms) allows to obtain the nominal conditions, by specifying nominal inputs. These conditions must be matched with those achieved at the end of the start-up of the boiler. The simulation of the reduced model has been built by Matlab software.

4.1. Fire/gas side

The thermal capacity effect of the combustion gas is neglected taking into account the rapid chemical combustion process with heat generation rate and a fast heat transfer process, in such a way that the values of these two terms are quite higher than the energy storage rate due to the thermal capacity effect of the combustion gas. Therefore, temperature changes are assumed to take place instantaneously for the flue gas.

- Mass balance

$$\text{Combustion chamber}: \dot{m}_{\text{fuel}} + \dot{m}_{\text{air}} = \dot{m}_g;\ V_g = V_H = V = \text{const.} \tag{36}$$

$$\text{Gas pass through a given tube bank},\quad j(j = 2, 3\ \text{y}\ 4): \dot{m}_g = \text{const.} \tag{37}$$

- Energy balance: Heat released to the water

$$\text{Maximum available}: \dot{m}_{\text{fuel}} LHV \tag{38}$$

$$\text{Heat release}: \dot{Q}_{g\to w} = \eta \dot{m}_{\text{fuel}} LHV \tag{39}$$

- Dynamics

The changes in energy of the water and metal are the physical phenomena that dominate the dynamics of the boiler [6]. For the metal, it will be used an average thermal capacitance defined as

$$CTM = \sum_{j=1}^{2,3,4} \rho_{t,j} V_{t,j} \overline{C}_{p,t,j} \tag{40}$$

The combustion chamber wall is exposed to very high temperatures. However, the metal temperature at steady-state condition is close to the steam temperature [18]. In any case, it is convenient to carry out an energy balance applied to the tubes of combustion chamber and the different gas passes, as follows:

$$CTM \frac{\mathrm{d}}{\mathrm{d}t}\overline{T}_{wall} = \left(\dot{Q}_{g\to w} - \sum_j \dot{q}_{j,water}\right) \tag{41}$$

$$\sum_j \dot{q}_{j,water} = \frac{A_{eq}}{\frac{R_{ext,t}}{\overline{k}_t}\ln\left(\frac{R_{ext,t}}{R_{ext,t} - e}\right) + \frac{1}{\overline{h}_{c,water}}}(\overline{T}_{wall} - T_{water}) = \xi(\overline{T}_{wall} - T_{water}) \tag{42}$$

$$A_{eq} = 2\pi\left[R_{ext,H} \cdot L_H + \sum_{j=2}^{4} n_{t,j} R_{ext,j} L_j\right] \tag{43}$$

$$CTM \frac{\mathrm{d}}{\mathrm{d}t}\overline{T}_{wall} = \left(\dot{Q}_{g\to w} - \xi(\overline{T}_{wall} - T_{water})\right) \Rightarrow \frac{CTM}{\xi}\frac{\mathrm{d}}{\mathrm{d}t}\overline{T}_{wall} + \overline{T}_{wall} = T_{water} + \frac{\dot{Q}_{g\to w}}{\xi} \tag{44}$$

In a cold start-up, $\overline{T}_{\text{wall}}$ $(t = 0)$ will be the ambient temperature. In a hot start-up, an updated temperature that accounts for the cooling, as $T(^\circ\text{C}) = T_{\text{shut-down}} - r_C \times t(\text{h})$, may be used, if a cooling rate of r_C °C/h is assumed or determined.

4.2. Water/steam side

Two parts are considered, one for each phase: steam and water.

- Dry steam (phase +)

It is assumed that the liquid phase is a saturated liquid. The model considers that exist a thermodynamic equilibrium between the liquid and vapor every time, i.e., vapor and liquid temperatures are the same. Thus, it is not necessary to establish an energy balance for the vapor phase. This hypothesis simplifies the problem although it remains close to the real case due to the sensible heat of the vapor is normally low compared to the latent heat. On the other hand, mass storage has a dynamics much faster than energy storage, because only steam is involved, and thus mass storage may be ignored when considering temperature dynamics.

$$\frac{\mathrm{d}}{\mathrm{d}t}m^+ = \dot{m}_v^- - \dot{m}_v^+ = 0 \Rightarrow \dot{m}_v^- = \dot{m}_v^+ \tag{45}$$

The expression of the volume fraction V^+ may be simplified as follows:

$$V^+ = A_l^+ L \cong 2RLl^+ - \frac{(4-\pi)}{2}R^2 L \to \frac{\mathrm{d}V^+}{\mathrm{d}t} = \frac{\mathrm{d}V^+}{\mathrm{d}l^+}\frac{\mathrm{d}l^+}{\mathrm{d}t} = 2RL\frac{\mathrm{d}l^+}{\mathrm{d}t} \tag{46}$$

that is very exact if the water level is not far from the middle of the shell.

- Saturated liquid water (phase −)

$$\frac{\mathrm{d}}{\mathrm{d}t}\left(\rho^- V^-\right) \approx \rho^- \frac{\mathrm{d}}{\mathrm{d}t}V^- = \dot{m}_f - \dot{m}_p - \dot{m}_v^- = \dot{m}_f - \dot{m}_p - \dot{m}_v^+ \tag{47}$$

$$V_{\text{total}} = V^- + V^+ = \text{const.} \Rightarrow \frac{dV^-}{dt} = -\frac{dV^+}{dt} \quad (48)$$

From Equations (46)–(48), using Equation (26) and taking into account that $P^+ = P^-$:

$$-2RL\rho^- \frac{d}{dt} l^+ = \dot{m}_f - \dot{m}_p - K_{VS} C^s f^s(x) \sqrt{(P - P_{\text{sum}})\rho_V} \quad (49)$$

$l^+(t = 0) = k_R R$ (k_R is a known constant corresponding to the initial steady-state level)

$$\dot{m}_v^+ = K_{VS} C^s f^s(x) \sqrt{(P - P_{\text{sum}})\rho_V} = K_{VS} C^s f^s(x) F_0(T) \quad (50)$$

since $P = P(T)$; $\rho = \rho(T)$, and

$$\rho V_{\text{total}} = \rho^-(T) V^- \left(l^+\right) + \rho^+(T) V^+ \left(l^+\right) \approx \rho^-(T) V^- \left(l^+\right) = F^* \left(T, l^+\right) \quad (51)$$

the global energy balance results in:

$$\frac{d}{dt} T \cong \frac{1}{\rho V_{\text{total}} \overline{C}_v} \left[\dot{m}_f \left(\overline{C}_{p,f} \left(T_f - T \right) \right) - K_{VS} C^s f^s(x) F_0(T) \overline{\lambda} + \sum_{j=1}^{2,3,4} \dot{q}_{j,\text{water}} - \text{Heat Losses} \right] \quad (52)$$

Table 1 exhibits the main energy/heat losses considered in the model expressed by efficiencies. Tables 2 and 3 include some additional equations and data for the fire/gas side and water/steam side, respectively, in order to solve the model.

4.3. Boiler start-up

It is assumed that the combustion begins just in the moment in which the fuel and air enter the boiler furnace. The fire/gas side is assumed to have a negligible dynamics, so only water/steam side is considered to be different respect to the model above described. With regarding to previous sections, the main change affects to the heat transfer in the water side, because the film coefficient for heat transfer is changing through the time. Therefore, this parameter must be upgraded (thus continuously increasing) as the boiler heats up, and it is shown in Table 3, where an ambient temperature of 20 °C and representative values normally used for natural convection and boiling [19] are considered. The film coefficient depends on latent heat, vapor density and temperature but, in line with that pointed out by other researchers [20], the value is so high that the final value is not too much important to calculate the wall temperature at a heat flux due to the corresponding resistance to heat transfer is very low. According to this, the approach for the convective film coefficient at nominal conditions (steady-state regime) has been taken.

For a hot start-up, i.e., when the temperature of shell is still high, it could be used the last temperature if the shut-down occurred not much time ago (a few minutes). A normal value for the cooling rate (r_C) of a big boiler is 20 °C/h, which helps to estimate the initial temperature.

The operation must be started with the air venting valve open and the steam valve closed. Next, the air venting valve will must be closed. This operation is not an easy task to model. Thus, when a boiler starts-up the majority of the gas contained will be air, not steam. In every moment, the boiler pressure will be the sum of that due to the air and the steam. This latter will be increasingly higher as the temperature and evaporation increase, thus decreasing the air pressure due to the air leaving the boiler through the venting and, hence, the shell pressure will be approached to the saturation. This process is very complex of solving, so some simplifications are adopted.

Table 1
Main losses considered by means of efficiencies.

Combustion gases to the chimney: $\frac{\dot{m}_g C_{p,g} (T_{g,\text{chim}} - T_{\text{ambient}})}{\dot{m}_{\text{fuel}} LHV}$

$C_{p,g} = 1$ kJ/(kg °C) or $C_{p,g} = (1.051 + 0.000114\, T_g)$ kJ/(°C kg)

Water blowdown: $\frac{\dot{m}_p C_{p,\text{water liq}} (T - T_{\text{ambient}})}{\dot{m}_{\text{fuel}} LHV}$

Moisture in the air: $\frac{\dot{m}_{\text{aire}} \frac{(RH(\%)/100) P_V(T_{\text{amb}}) M_{H_2O}}{P_{\text{atm}} M_{\text{air}}} C_{p,v} (T_{g,\text{chim}} - T_{\text{amb}})}{\dot{m}_{\text{fuel}} LHV}$;

$P_v(T) = 10^{\left[5.0844 - \frac{1668.7166}{T(K) - 45}\right]}$ (bar)

This loss is accounted for the losses of the gases flowing through the chimney.

By radiation and convection, given by a coefficient α that is a function of the load and the size of the boiler (% of $\dot{m}_{\text{fuel}} LHV$):

$P_{r-c} = \alpha \cdot \dot{m}_{\text{fuel}} \cdot LHV$; $\alpha = \alpha(\text{boiler, load})$

where % load is the % rate of firing, Thus, representing load − energy loss,[a] for a boiler of 800 HP:

25–1.2%; 50–0.6%; 75–0.4%; and 100–0.3%

Or by applying the Spanish standard UNE-EN 12953-11:2004, these losses can be accounted by $P_{r-c} = 0.0072\, \dot{Q}_E^{0.6}$, where $\dot{Q}_E$ is the estimated useful thermal power, in MW, i.e., $\eta\, \dot{m}_{\text{fuel}} LHV$

Although there is other kind of losses, those above cited are the most representative ones.

[a] www.boilerspec.com/EmmisEffic/boiler%5fefficiency%5ffacts.pdf.

Table 2
Additional data and expressions for the fire/gas side.

Fuel-oil characteristics[a]:
Carbon, % w (C): 86.6
Hydrogen, % w (H): 10.9
Sulfur, % w (S): 2.1
Ash, % w: 0.4
LHV, MJ/kg: 39.4
Theoretical air/fuel ratio (A/F):

$A/F)_t = \frac{m_{\text{air}}}{m_{\text{fuel}}} = 11.45\, C + 34.33\, H + 4.29\, S (\text{kg}_{\text{air}}/\text{kg}_{\text{fuel}})$

$\dot{m}_{\text{air}})_{t,\text{dry}} = A/F)_t \dot{m}_{\text{fuel}}$

$\dot{m}_{\text{air}})_{t,\text{wet}} = \dot{m}_{\text{aire}})_{t,\text{dry}} \cdot \left(1 + \frac{RH(\%)/100 \cdot P_v(T_{\text{amb}}) \cdot M_{H_2O}}{(P_{\text{amb}} - P_v) \cdot M_{\text{dry air}}}\right)$

By considering the air excess (AE):

$A/F)_{\text{real}} = AE \times A/F)_t (\text{kg}_{\text{aire}}/\text{kg}_{\text{fuel}})$

$AE = \frac{\dot{m}_{\text{air}})_{\text{real,wet}}}{\dot{m}_{\text{air}})_{t,\text{wet}}} = \frac{\text{kg}_{\text{air,real}}}{\text{kg}_{\text{aire},t}}$

$\dot{m}_{\text{air}})_{\text{real,wet}} = AE \times A/F)_t \times \dot{m}_{\text{fuel}} \cdot \left(1 + \frac{RH(\%)/100 \cdot P_v(T_{\text{amb}}) \cdot M_{H_2O}}{(P_{\text{amb}} - P_v) \cdot M_{\text{dry air}}}\right)$

Oxygen concentration in the flue gases to the chimney (dry-basis):

$O_2(\%\text{vol})_{\text{dry basis}} = \frac{n_{O_2}}{n_{N_2} + n_{g,s} + n_{O_2}} \times 100$

$n_{O_2} = (AE - 1) \times (C/12 + 0.5\, H + S/32)$
$n_{N_2} = 79/21 \times AE \times (C/12 + 0.5\, H + S/32)$
$n_{g,s} = (C/12 + S/32)$
n is the molar flow-rate

Oxygen concentration in the flue gases to the chimney (wet basis)

$O_2(\%\text{vol})_{\text{wet basis}} = \frac{n_{O_2}}{n_{N_2} + n_{g,s} + n_{O_2} + n_{H_2O}} \times 100$

$n_{H_2O} = 0.5\, H + 100/21 \times AE \times (C/12 + 0.5\, H + S/32) \times \frac{RH(\%)/100 \times P_v(T_{\text{amb}})}{P_{\text{amb}} - P_v}$

Expressions valid by assuming a complete combustion.

[a] www.boilerspec.com/EmmisEffic/boiler_efficiency_facts.pdf.

Table 3
Additional data and expressions for the water/steam side.

$$P = \exp\left(\frac{T-99.63}{T+273}\left[12.7+\left(\frac{374-T}{339.6}\right)^{2.174}\right]\right);\ P \text{ in bar and } T \text{ in } ^\circ\text{C}$$

$$\bar{h}_{c,\text{water}} = 12+\alpha_{h1}\cdot 2.18\cdot(T-25)+\alpha_{h2}\cdot(175+98.33\cdot(T-100))+\alpha_{h3}\cdot h_{nb}\ \text{kJ}/(h\cdot\text{m}^2\cdot^\circ\text{C})$$

$\alpha_{h1} = 1$ if $25 \le T \le 100^\circ C$; $\alpha_{h1} = 0$ for another T

$\alpha_{h2} = 1$ if $100 < T \le 110^\circ C$; $\alpha_{h2} = 0$ for another T

$\alpha_{h3} = 1$ if $T > 110^\circ C$; $\alpha_{h3} = 0$ for another T

where the Cooper pool boiling correlation is used

$$h_{nb} = 12.96 p_r^{0.12}(-0.4343\ln p_r)^{-0.55}(Q/A)^{0.67}$$

The heat flux (Q/A) is in W/m^2. For a range of pressures from 2 to 15 bar, and using fuel-oil with the nominal fuel flow-rate, h ranges from 4260 to 7419 W/m^{2}K.

- Air − dry steam in the upper zone (phase +)

It is assumed that the air is vented by the vapor that is being generated during the start-up and heat-up processes, although without losing steam. In any time, thermodynamic equilibrium is considered between the lower and upper zones. When the venting valve is open, $f^{\text{air}}(x) = 1$. The steam valve is closed while the air venting valve is open. Likewise, the steam valve should not be opened until achieving the operating pressure and temperature set.

- If $f^{\text{air}}(x) = 1 \Rightarrow$ open venting $\Rightarrow \beta_1 = 1$(start − up)
- If $f^{\text{air}}(x) = 0 \Rightarrow$ closed venting $\Rightarrow \beta_1 = 0$(start − up)
- If $f^{s}(x) = 0 \Rightarrow$ steam out of service $\Rightarrow \beta_2 = 0$(start − up)
- If $f^{s}(x) > 0 \Rightarrow$ steam on service $\Rightarrow \beta_2 = 1$(start − up → nom)

$$\begin{aligned}\frac{\mathrm{d}}{\mathrm{d}t}m^+ &= \frac{\mathrm{d}}{\mathrm{d}t}(\beta_1 m_{\text{air}} + m_v)\\ &= \dot{m}_v^- - (1-\beta_1)\cdot\beta_2\cdot\dot{m}_v^+ - \beta_1\cdot(1-\beta_2)\dot{m}_{\text{air},p}\end{aligned} \tag{53}$$

$$\begin{aligned}&\text{If } \beta_1 = 1 \text{ and } \beta_2 = 0 \ \text{(start − up)} \Rightarrow \dot{m}_v^+ = 0; \Rightarrow \frac{\mathrm{d}}{\mathrm{d}t}m_v\\ &\quad = \dot{m}_v^- - \dot{m}_v^+ = \dot{m}_v^-;\end{aligned} \tag{54}$$

and

$$\frac{\mathrm{d}}{\mathrm{d}t}(m_{\text{air}}) = -\dot{m}_{\text{air},p} \tag{55}$$

$$\text{with } m_{\text{air}}(t=0) = \frac{P_{\text{air}}V^+M_{\text{air}}}{R_g T_{(t=0)}} = \frac{P_{\text{amb}}V^+M_{\text{air}}}{R_g T_{(t=0)}}$$

$$\text{If } \beta_1 = 0 \text{ and } \beta_2 = 0 \text{(start − up)} \Rightarrow m_{\text{aire}} = 0;\ \dot{m}_{\text{air},p} = 0 \tag{56}$$

$$\dot{m}_v^+ = 0;\ \frac{\mathrm{d}}{\mathrm{d}t}m_v = \dot{m}_v^- - \dot{m}_v^+ = \dot{m}_v^- \tag{57}$$

$$\begin{aligned}&\text{If } \beta_2 = 1 \text{ and } \beta_1 = 0 \text{(start − up → nom)} \Rightarrow \frac{\mathrm{d}}{\mathrm{d}t}m^+ = \dot{m}_v^- - \dot{m}_v^+\\ &\quad = 0 \Rightarrow \dot{m}_v^- = \dot{m}_v^+\end{aligned} \tag{58}$$

$$\begin{aligned}\dot{m}_{\text{air},p} &= K_{VS}^{\text{air}} C^{\text{air}} f^{\text{air}}(x)\sqrt{(P-P_{\text{atm}})\rho_a}\\ &= K_{VS}^{\text{air}} C^{\text{air}} f^{\text{air}}(x)\sqrt{(P_v(T)+P_{\text{air}}(T)-P_{\text{amb}})\rho_{\text{air}}}\\ &= K_{VS}^{\text{air}} C^{\text{air}} f^{\text{air}}(x)\sqrt{\left(P^-(T)+\frac{m_{\text{air}}R_gT}{M_{\text{air}}V^+}-P_{\text{amb}}\right)\frac{m_{\text{air}}}{V^+}}\\ &= K_{VS}^{\text{air}} C^{\text{air}} f^{\text{air}}(x) F_1(m_{\text{air}}, T)\end{aligned} \tag{59}$$

where C^{air} and $f^{\text{air}}(x)$ are a conversion factor of units and the inherent characteristic for the air venting valve, respectively. Likewise, Equation (50) is used for the steam, with a constraint for $P_{\text{sum}}: P - P_{\text{sum}} \ge 0$.

The above expressions allow to obtain the mass flow-rates through the air venting valve and the steam control valve. The logic sequence implies that first β_1 must be 1 and β_2 must be 0, and finally, once the boiler is providing steam to consumers, β_1 must be 0 and β_2 must be 1. Thus,

$$\frac{\mathrm{d}}{\mathrm{d}t}m^+ = \dot{m}_v^- - \beta_2\cdot\dot{m}_v^+ - \beta_1\cdot\dot{m}_{\text{air},p} \tag{60}$$

Using Equation (46):While

$$\begin{aligned}\beta_2 = 0,\quad \dot{m}_v^- &= \frac{V^+M_{H_2O}}{R_g}\frac{\mathrm{d}}{\mathrm{d}t}(P_v(T)/T) = \frac{V^+M_{H_2O}}{R_g}\frac{\mathrm{d}}{\mathrm{d}t}(F_2(T))\\ &= \frac{V^+M_{H_2O}}{R_g}\frac{\mathrm{d}F_2(T)}{\mathrm{d}T}\frac{\mathrm{d}T}{\mathrm{d}t}\end{aligned} \tag{61}$$

- Saturated liquid in the lower zone (phase −)

$$\frac{\mathrm{d}}{\mathrm{d}t}\left(\rho^-V^-\right) \approx \rho^-\frac{\mathrm{d}}{\mathrm{d}t}V^- = \dot{m}_f - \dot{m}_p - \dot{m}_v^- \tag{62}$$

$$\begin{aligned}\frac{\mathrm{d}V^-}{\mathrm{d}t} &= -\frac{\mathrm{d}V^+}{\mathrm{d}t} \Rightarrow -2RL\rho^-\frac{\mathrm{d}}{\mathrm{d}t}l^+\\ &= \dot{m}_f - \dot{m}_p - \frac{V^+M_{H_2O}}{R_g}\cdot\frac{\mathrm{d}F_2(T)}{\mathrm{d}T}\cdot\frac{\mathrm{d}T}{\mathrm{d}t}\end{aligned} \tag{63}$$

$l^+(t=0) = k_R R$ (k_R is a known constant corresponding to the initial steady-state level).

Table 4
Additional elements in a fire-tube boiler system.

Component	Equations	Comments
Economizer	$\dot{m}_g \overline{C}_{p,g,EC}(T_{\text{in},g,EC} - T_{\text{out},g,EC}) = Q_{\text{wall},EC}$ $m_{t,EC}\overline{C}_{p\ t,EC}\dfrac{dT_{t,EC}}{dt} = Q_{\text{wall}} - Q = \dot{m}_g \overline{C}_{p\ g,EC}(T_{\text{in},g,EC} - T_{\text{in},g,EC}) - Q$ $\dot{m}_f \overline{C}_{p\ \text{water},EC}(T_{\text{out,water},EC} - T_{\text{in,water},EC}) = Q - Pd_{EC}$ $Pd_{EC} = 0$ except changes due to a disturb $Q = k_{c,\text{water}}\dot{m}_f^{0.8}(T_{\text{wall},EC} - T_{\text{water}})$; estimating $k_{c,\text{water}} = 2$; $\dot{m}_f$ in kg/h $\overline{T} = \dfrac{T_{\text{in}} + T_{\text{outl}}}{2}(^\circ\text{C})$; $\overline{\rho} = \dfrac{\rho_{\text{in}} + \rho_{\text{out}}}{2}$ (for the gas)	In the model, it is assumed that both the gas and the water have a negligible dynamics from the energy point of view and, when the operating conditions change, storage terms are for the metal tube wall that provides the area for heat transfer. The maximum achievable heating value depends on the minimum chimney temperature, which should be higher than the acid dew point. $m_{t,EC}\overline{C}_{p\ t,EC}$ is estimated to be 500 kJ/°C, in this case. The equation for Q (heat transferred from metal walls to water) is taken from Refs. [21,27,28].
Superheater	$\eta_{SH}\,\dot{m}_{\text{fuel}}LHV = Q_{\text{wall}}$; $j = 1,\ldots,4$ $m_{t,SH}\overline{C}_{p\ t,SC}\dfrac{dT_{t,SH}}{dt} = Q_{\text{wall}} - Q = \eta_{SH}\,\dot{m}_{\text{fuel}}LHV - Q$ $\dot{m}_v^+ \overline{C}_{p\ v,SH}(T_{\text{out},SH} - T^+) = Q - Pd_{SH}$ $T^+ = T_{\text{in},SH} = T_{\text{saturation}}(P_{\text{boiler}})$; T in °C $Pd_{SH} = 0$ except changes due to a disturb $Q = k_{c,v}\dot{m}_v^{0.8}(T_{\text{wall},SH} - T_v)$; estimating $k_{c,v} = 0.8$; $\dot{m}_v$ in kg/h $\overline{T} = \dfrac{T_{\text{in}} + T_{\text{out}}}{2}$; $\overline{\rho} = \dfrac{\rho_{\text{in}} + \rho_{\text{out}}}{2}$ (steam and gas)	In case of only using a superheater, a set of equations similar to that used for economizer would reduce the problem. The superheater is normally located in the upper part of the furnace, where the temperatures are still quite high. It is a single-phase heat exchanger with steam flowing inside the tubes and flue gas passing outside. It can be approached by a fraction of the heat release in furnace. $m_{t,SC}\overline{C}_{p\ t,SH}$ is estimated to be 2300 kJ/°C in this case. The equation for Q (heat transferred from metal walls to steam) is taken from Refs. [21,27,28]. Storage term in the flow equation is neglected. Clearly, the maximum achievable heating value depends on the enthalpy difference of the combustion gas stream. This option is not as common in fire-tube boilers as they are in water-tube boilers.
Attemperator	$\dot{m}_{\text{out},ATT} = \dot{m}_v^+ + \dot{m}_{\text{spray}}$ $\dot{m}_{\text{out},ATT}h_{\text{out}} = \dot{m}_v^+ h_{\text{out},SH} + \dot{m}_{\text{spray}}h_{\text{spray}}$ $T_{\text{out},ATT} = \dfrac{\dot{m}_v^+ \overline{C}_{p\ v,SH}T_{\text{out},SH} + \dot{m}_{\text{spray}}C_{P,f}T_{\text{spray}} - \dot{m}_{\text{spray}}\overline{\lambda}}{(\dot{m}_v^+ + \dot{m}_{\text{spray}})\cdot\overline{C}_{p\ v,SH}}$, or $\dot{m}_{\text{spray}} = \dfrac{\dot{m}_v^+ \overline{C}_{p\ v,SH}(T_{\text{out},SH} - T_{\text{out},ATT})}{(\overline{C}_{p\ v,SH}T_{\text{out},ATT} + \overline{\lambda}) - C_{P,f}\cdot T_{\text{spray}}}$ $T_{\text{spray}} \approx T_f$ $Pd_{ATT} \approx 0$	The attemperation carried out by a water spray is a method to control the temperature for superheated steam, by atomizing liquid water that is evaporated inside. The water spray is modulated by a suitable valve. Because the attemperator has a relatively small volume, the mass and heat storages inside that are negligible. The value for $C_{pv,SH}$ is evaluated at the average temperature between $T_{\text{out},SC}$ (at the attemperator inlet) and $T_{\text{out},ATT}$ (at the attemperator outlet). The spray is liquid water at temperature of feeding water, which is atomized and evaporated to obtain a wished superheated steam temperature. The sprayed water flow-rate will be the manipulated variable in order to control a wished outlet temperature for the steam.
Blowdown heat recovery Stage 1	Simple flash Mass balance : $\dot{m}_p = \dot{m}_{V,\text{flash}} + \dot{m}_{L,\text{flash}}$ Energy balance : $\dot{m}_p\cdot h_p = \dot{m}_{V,\text{flash}}\cdot h_{V,\text{flash}} + \dot{m}_{L,\text{flash}}\cdot h_{L,\text{flash}} + Pd_{\text{flash}}$ $Pd_{\text{flash}} = 0$ except change due to a disturb $\dfrac{\dot{m}_{V,\text{flash}}}{\dot{m}_p} = \dfrac{\overline{C}_{p,L}(T_p - T_{\text{flash}})}{\overline{\lambda}}$; $T_{\text{flash}} = T_{\text{flash}}(P_{\text{flash}})$	The blowdown water from the boiler can be addressed to an expansion tank where flash vapor is produced if the pressure is diminished. The minimum pressure at the outlet of the boiler can be set in 3 bar, so the pressure of the flash steam is of 1.5 bar, i.e., the water will expand from the boiler pressure to 1.5 bar. The tank normally has a small volume so the dynamics will be negligible relative to its heating (the value of $m_{t,EC} \times Cp_{t,EC}$ is quite lower than that of the boiler tubes and furnace). Besides, it is assumed that the blowdown enters the flash separator at pressure and temperature of the boiler, and the steam and water are in equilibrium at the temperature corresponding to the pressure at which the blowdown is expanded.
Blowdown heat recovery Stage 2	Water–water heat exchanger $\dot{m}_{L,\text{flash}}\cdot h_{L,\text{flash}} + \dot{m}_{\text{make-up}}\cdot h_{\text{make-up,in}} = \dot{m}_{L,\text{flash}}\cdot h_{L,\text{deg}} + \dot{m}_{\text{make-up}}\cdot h_{\text{make-up,out}} + Pd_{IC}$ $\dot{m}_{L,\text{flash}}\cdot\overline{C}_{p,L}\cdot(T_{\text{flash}} - T_{\text{deg}}) - Pd_{IC} = \dot{m}_{\text{make-up}}\cdot\overline{C}_{p,L}\cdot(T_{\text{make-up,out}} - T_{\text{make-up,in}})$ $(1 - f_{Pd_{IC}})\cdot\dot{m}_{L,\text{flash}}\cdot\overline{C}_{p,L}\cdot(T_{\text{flash}} - T_{\text{deg}}) = \dot{m}_{\text{make-up}}\cdot\overline{C}_{p,L}\cdot(T_{\text{make-up,out}} - T_{\text{make-up,in}})$ $T_{\text{make-up,out}} = T_{\text{make-up,in}} + \dfrac{(1 - f_{Pd_{IC}})\cdot\dot{m}_{L,\text{flash}}\cdot\overline{C}_{p,L}\cdot(T_{flash} - T_{\text{deg}})}{\dot{m}_{\text{make-up}}\cdot\overline{C}_{p,L}} \cong$ $\cong T_{\text{make-up,in}} + \dfrac{(1 - f_{Pd_{IC}})\cdot\dot{m}_{L,\text{flash}}\cdot(T_{\text{flash}} - T_{\text{deg}})}{\dot{m}_{\text{make-up}}}$ $\dot{m}_{\text{make-up}} = \dot{m}_f$	The liquid water from the flash separator may be used for preheating the water feeding by a heat exchanger before going into the degasifier. In this case, it will be assumed that the dynamics of the heat exchanger walls can be neglected. The operation may be set so as to have a temperature of water discharge from the flash stage of 5 °C more than that of the water input, which is an input variable. Heat losses have been expressed as a fraction of the enthalpy difference for the heat fluid through the factor, f_{PdIC}, which is a configuration parameter (input data of the model).
Degasifier	$\dot{m}_{\text{make-up}} + \dot{m}_{\text{cond}} + \dot{m}_{V,\text{flash}} = \dot{m}_f + \dot{m}_{\text{gases,deg}}$ $\dot{m}_{\text{make-up}}\cdot h_{\text{make-up,out},IC} + \dot{m}_{\text{cond}}\cdot h_{\text{cond}} + \dot{m}_{V,\text{flash}}\cdot h_{V,\text{flash}} = \dot{m}_f\cdot h_f$ $T_f = \dfrac{\dot{m}_{\text{make-up}}\cdot\overline{C}_{p,L}\cdot T_{\text{make-up,out},IC} + \dot{m}_{\text{cond}}\cdot\overline{C}_{p,L}\cdot T_{\text{cond}} + \dot{m}_{V,\text{flash}}\cdot(\overline{C}_{p,V}\cdot T_{\text{make-up,out},IC} + \overline{\lambda})}{\dot{m}_{\text{make-up}} + \dot{m}_{\text{cond}} + \dot{m}_{V,\text{flash}}} =$ $= \dfrac{\dot{m}_{\text{make-up}}\cdot\overline{C}_{p,L}\cdot T_{\text{make-up,out},IC} + \dot{m}_{\text{cond}}\cdot\overline{C}_{p,L}\cdot(T_v^+ - 10) + \dot{m}_{V,\text{flash}}\cdot(\overline{C}_{p,V}\cdot T_{\text{make-up,out},IC} + \overline{\lambda})}{\dot{m}_{\text{make-up}} + \dot{m}_{\text{cond}} + \dot{m}_{V,\text{flash}}}$ $\dot{m}_{\text{make-up}} = \dot{m}_f$ $Pd_{\text{DEG}} \approx 0$	In the thermal degasifier, the dissolved gases in water are removed, especially oxygen and carbon dioxide that corrode the metal in the water side of the boiler. From all the phenomena occurring in the degasifier, only those related directly to the energy balance have been taken into account. The streams entering this equipment are the condensed water collected from those points in which saturated steam has been used, the make-up water and the steam coming from the flash separator. The outlet streams are the removed gases (neglected in the energy balance) and the feed water of the boiler. No heat losses to the ambient have been assumed. Although the model does not include the condensed vapor unit, it can be assigned a value of condensed water flow-rate as a function of the feed water of the boiler. Condensed water is collected in a tank and from this it flows to the degasifier. As an approach, it may be assumed that condensed water has a temperature around 10 −15 °C less than operating temperature inside the boiler.

The global energy balance including the two zones is:

$$\frac{\mathrm{d}}{\mathrm{d}t}T \cong \frac{\beta_1(1-\beta_2)}{\rho^-(T)V^-\left(l^+\right)\overline{C}_v^- + \bar{\lambda}\frac{\bar{V}^+M_{H_2O}}{R_g}\frac{\mathrm{d}F_2(T)}{\mathrm{d}T}}\left[\begin{array}{l}\dot{m}_f\left(h_f\left(T_f\right)-h^-(T)\right)+\sum_{j=1}^{2,3,4}\dot{q}_{j,\mathrm{water}}\\ -K_{VS}^{\mathrm{air}}C^{\mathrm{air}}f^{\mathrm{air}}(x)F_1(m_{\mathrm{air}},T)\left(h_a(T_a)-h^-(T)\right)\end{array}\right]$$
$$+\frac{(1-\beta_1)(1-\beta_2)}{\rho^-(T)V^-\left(l^+\right)\overline{C}_v^- + \bar{\lambda}\frac{\bar{V}^+M_{H_2O}}{R_g}\frac{\mathrm{d}F_2(T)}{\mathrm{d}T}}\left[\dot{m}_f\left(h_f\left(T_f\right)-h^-(T)\right)+\sum_{j=1}^{2,3,4}\dot{q}_{j,\mathrm{water}}\right]$$
$$+\frac{(1-\beta_1)\beta_2}{\rho V_{\mathrm{total}}\overline{C}_v}\left[\dot{m}_f\left(h_f\left(T_f\right)-h^-\left(T^-\right)\right)+\sum_{j=1}^{4}\dot{q}_{j,\mathrm{water}}-K_{VS}C^sf^s(x)F_0(T)\bar{\lambda}\right]+\frac{1}{\rho V_{\mathrm{total}}\overline{C}_v}\text{Heat Losses} \quad (64)$$

where it has been used Equation (51).

The water specific volume depends on the temperature [21]:

$$1/\rho^- = v^- = 0.001 + 5.82\times10^{-9}T^{1.93}\left(\mathrm{m}^3/\mathrm{kg}\right)$$

So, by rearranging the energy balance equation, it turns out:

$$\frac{\mathrm{d}}{\mathrm{d}t}T \cong \frac{(1-\beta_2)}{\rho^-(T)V^-\left(l^+\right)\overline{C}_v^- + \bar{\lambda}\frac{\bar{V}^+M_{H_2O}}{R_g}\frac{\mathrm{d}F_2(T)}{\mathrm{d}T}}\left[\begin{array}{l}\dot{m}_f\left(h_f\left(T_f\right)-h^-\left(T^-\right)\right)+\sum_{j=1}^{2,3,4}\dot{q}_{j,\mathrm{water}}\\ -\beta_1K_{VS}^{\mathrm{air}}C^{\mathrm{air}}f^{\mathrm{air}}(x)F_1(m_{\mathrm{air}},T)\left(h_a(T_a)-h^-\left(T^-\right)\right)\end{array}\right]+\frac{(1-\beta_1)\beta_2}{\rho V_{\mathrm{total}}\overline{C}_v}\left[\dot{m}_f\left(h_f\left(T_f\right)-h^-\left(T^-\right)\right)\right.$$
$$\left.+\sum_{j=1}^{4}\dot{q}_{\mathrm{conv},j,\mathrm{water}}-K_{VS}C^sf^s(x)F_0(T)\bar{\lambda}\right]+\frac{1}{\rho V_{\mathrm{total}}\overline{C}_v}\text{Heat Losses} \quad (65)$$

Thus, all the energy transferred by the gases will be used in heating the entering water and to increase the temperature (and pressure) in the water side of the boiler until achieving the wished value, just before opening the steam control valve, and the first term of the energy balance is applied. When this situation is reached, the equations of the model corresponding to the nominal operation will be valid again, and then it must be used the second term just as it was shown in the previous section. Obviously, heat losses must be always accounted for.

Some additional elements may be included in the model as an economizer, superheater, attemperator, energy use of blowdown and degasifier in order to complete the model as parts of the fire-tube boiler. The modeling proposed for these components is shown in Table 4, in order to condense the extent of this paper. In this table, it is considered that the energy content of the water blowdown from the boiler may be recovered by flashing the blowdown in an expansion tank and then using the generated saturated steam in a thermal degasifier as a heat transfer fluid. Besides, the liquid water of the tank's lower zone may be used for preheating the water feeding through a heat exchanger.

5. A simulated case-study

The model proposed uses some assumptions to reduce the computational complexity but still providing realistic results. Thus, it is necessary to check the accuracy of the predictions against direct experimental data or literature references. For the verification of the rightness of the model, at least qualitative results should be agree well with experimental values or previously published values. The objective of the case-study simulation is to estimate the suitability of the model qualitatively. There is a lack of published results of modeling and experimental tests carried out in a fire-tube boiler, but finally some references have been taken from the literature so as to contrast the model results.

The overall calculation scheme for the complete model is shown in Fig. 6. The fire-tube boiler model has been simulated using Matlab. Before running the simulation, all the constants and parameters such as boiler geometry and configuration including valves and the possible additional elements, or heating value and moisture content of the fuel and ambient conditions, are set. The simulation starts once the boiler is ready and so the fuel and air are entered as well as the feed water, following the model. When the convergence is achieved and wished steady state is matched, some changes can be carried out to get the dynamic behavior of the boiler while a new steady state may be reached.

In order to validate the performance of the modeling approach, some running tests are performed under various situations from a case study. Next, some simulation results will be obtained and then compared with test results from the literature. As an example and case study, an 800 HP fire-tube boiler has been selected for testing the model. Table 5 shows the data of the real boiler chosen for carrying the simulation and Table 6 includes the steady-state operating conditions of the simulated boiler.

To make possible a comparison with available data the additional elements considered in Table 4 are not taken into account, and thus only the boiler itself has been simulated: fire/gas side and water/steam side.

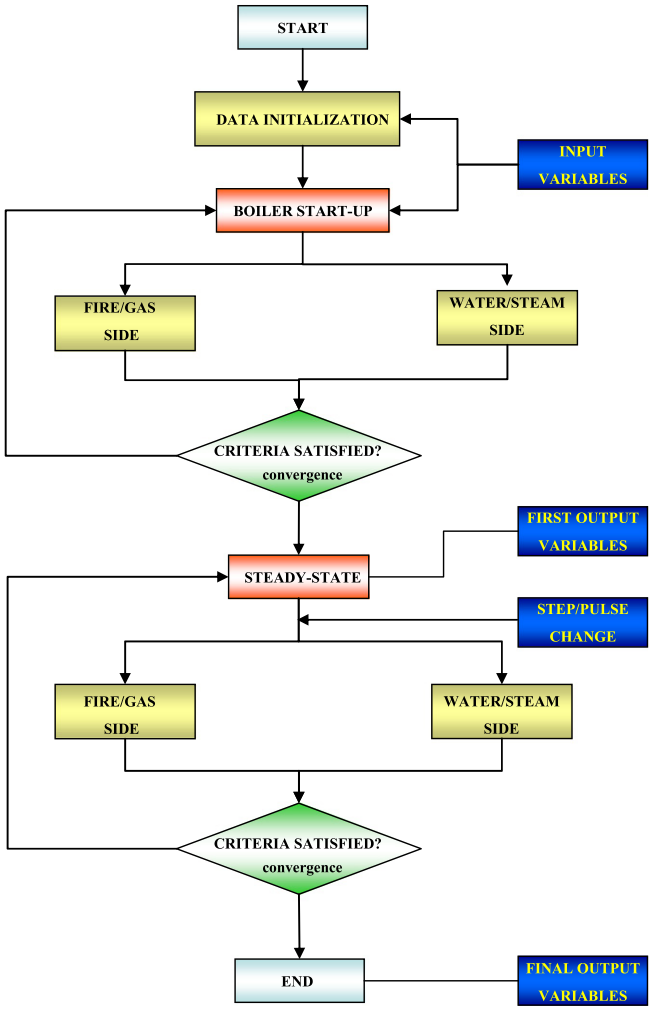

Fig. 6. Overall calculation scheme of the complete model.

Table 6
Steady-state operating conditions of the case-study simulated.

Parameters	Values
Boiler/Steam temperature	471.0 K
Steam pressure	15.0 bar
Steam flow-rate	3600.0 kg/h
Water level	2.48 m
Water volume	17.98 m^3
Feed water flow-rate	3672.0 kg/h
Water purge	72.0 kg/h
Feed water temperature	126.0 °C
Fuel flow-rate (fuel-oil)	792.0 kg/h
Fuel temperature	105.0 °C
Oxygen in flue gas	4.0 %vol
Air flow-rate	12816.0 Nm^3/h (@273 K, 1 atm)
Flue-gas flow-rate	17280.0 kg/h
Flue gas temp2erature chimney	213.0 °C
Ambient conditions:	
Temperature	293 K
Pressure	1 bar
Relative humidity	30%

The open loop transient response of the chosen boiler is simulated when a pulse change is made to one of the two more relevant factors, but being the oxygen present in the flue gas under control: the *heating rate (fuel flow-rate)* and the *steam demand* (*steam flow-rate*).

As aforementioned, the main input variables are fuel, air, feed water flow-rates and steam valve opening, as well as fuel, air and feed water temperatures. Reaction of steam pressure, steam flow-rate, water/steam side temperature and water volume will be illustrated.

The simulation process first runs until reaching a steady state. Then, for some time, the steady state is represented, and at a given moment, fuel-oil flow-rate or steam valve opening (and, hence, steam flow-rate) is suddenly increased (by a pulse or step change), and that value is then maintained for some time. During this time, output variables are changing. Next, the situation is replaced at its

Table 5
Data of an 800 HP fire-tube boiler (horizontal packaged four-pass fire-tube boiler).

	Fire side	Water side
A_{eq} (m^2)	325.16	353.96
Boiler radius (m)	1.480	
Length (m)	6	
Max. operating pressure (bar)	20	
Max. steam flow-rate (kg/h)	12602	
Chimney temperature (°C)	$T_{g,chim} = 149.0 + 4.78 \cdot P_{boiler}$	
η_{FS} (@1.7 bar) (%)	89.8	
$\eta_{FS}(\%) = \eta_{FS(@1,7\ bar)}(\%) - Co \cdot ([O_2]_{out,dry-basis} - 3) + 0,027 \cdot (T_{air} - 25) - 0,35 \cdot (P_{boiler} - 1.7)$[a]		
where:		
$[O_2]_{out,\ dry\text{-}basis}$:0–3% v →Co = 0.33		
$[O_2]_{out,\ dry\text{-}basis}$:3 y 6% v →Co = 0.43		
$[O_2]_{out,\ dry\text{-}basis}$:6 y 8% v →Co = 0.60		
$[O_2]_{out,\ dry\text{-}basis}$:8 y 10% v →Co = 1.50		
$[O_2]_{out,\ dry\text{-}basis}$:> 10% v →Co = 2.00		
T_{air} (inlet) in °C, and P_{boiler} (operating pressure) in bar.		
CTM (kJ/°C)	6503.2	
ρ_t (kg/m^3)	8000	
$C_{p,t}$ (kJ/(kg °C))	0.5	
$\overline{k}_t$ (kJ/(hm °C))	170	
$\overline{e}$ (mm)	5	
K_{VS}^{vapor}[b]	800	
K_{VS}^{air}	5.0	

Reference: www.boilerspec.com (many data have been taken from this Web link).

[a] *Fuel-To-Steam Efficiency*, η_{FS}, is the fraction of available energy used to generate steam. Between 25 and 100% of the boiler load, the efficiency does not change significantly (about 0.2%), so η_{FS} will be considered as independent of the boiler load. This efficiency is $\eta_{FS} = f$(*fuel*, m_{air},T_{amb}, boiler, vapor pressure).

[b] the maximum pressure drop (for an operating pressure of 21 bar) is 18.2 bar $f(x) = x$, $0 \le x \le 1$; x is the valve opening.

original state by performing another step opposite to the first one, so as to output variables tend to their original steady state values.

Fig. 7 gives the evolution curves of some main parameters in the water/steam of the boiler for a pulse change in the heating rate (fuel flow-rate) as above described. The air flow-rate for combustion is manipulated in such a way that oxygen concentration at the outlet of chimney to be about 4 %vol. When the fuel-oil feed rate increases suddenly, more heat is absorbed by the transfer walls, so the pressure of the steam inside the boiler increases correspondingly as well as the steam flow-rate. The change in steam temperature is related to heat transfer and steam flow-rate. When the fuel-oil rate decreases suddenly, the opposite phenomenon is observed.

Fig. 8 gives the evolution curves of the same parameters shown in previous figure, but changing the steam demand (steam flow-rate) by varying the steam valve opening. In this case, the fuel flow-rate and the air flow rate are kept constant.

The results in Figs. 7 and 8 show the dynamic behavior of some boiler output variables, and there is a good qualitative agreement between the model and the experimental data from literature [22–24], except for the swell phenomenon not accounted for this kind of boiler as aforementioned (±3–4 cm measured variation). Huang and Ko [22] used a half-ton fire-tube shell boiler installed in a laboratory for the experiment in their study. They pre-filtered data before system identification since the testing signals could be corrupted by internal and external disturbances or noises. In the present study, no noise has been considered. The tests in Ref. [22] were run at six different operating conditions with the fuel flow-rate ranging from 14.6 to 37.9 kg/h; the water flow-rate ranging from 181 to 465 kg/h; the steam pressure ranging from 3.8 to 7.3 kg/cm^2 gage. Sørensen et al. [23] as well as Karstensen et al. [24] used a boiler applied for the experiments is an Aalborg Industries boiler type Mission™ OB, a bottom-fired fire-tube boiler for light and heavy fuel-oil. Sørensen et al. [23] carried out a step-input on fuel flow-rate from 80 to 230 kg/h during about 400 s. They got an almost linear increase in the steam pressure from 6 to 8 bar, without a significant dead time. Besides, the steam flow-rate increased from 750 to 1250 kg/h, in a nearly linear way. Karstensen et al. [24] carried out tests at 50 percent load with pressure at 7 bar. When a fuel flow-rate step was made the steam pressure increased from 6 to 8 bar in 150 s and when a steam flow-rate was changed by closing the steam valve, the steam pressure increased from 5.5 to 8.5 bar for about 700 s.

Rodriguez Vasquez et al. [25] carried out an experiment with step-signal input in fuel valve opening recording the output studied (steam pressure) with the aim of obtaining the dynamic behavior of the boiler regarding these two variables. They collected data from a laboratory-scale fire-tube boiler. The main characteristics of this boiler are a total length of 2.65 m, body diameter of 1.10 m height of 1.60 m, operation pressure of 250 kPa, generated steam flow-rate of 80 kg/h and three passes of combustion gases passes. Fig. 9 illustrates a similar qualitative behavior respect this previous work. During this step experiment, the feed water must be fed into the boiler to match the production of steam so as to keep the level under control. As it can be seen, firstly the steam pressure increases quickly, but the system is self regulating and over the time the outputs achieve a new steady state, just as in the study of these researchers.

Fig. 10 illustrates the boiler performance during the start-up from the beginning until reaching a steady state close to that shown in Table 6. In this case, the final boiler pressure is 14.67 bar, and the steam flow-rate is 3650 kg/h. The first stage is a boiler

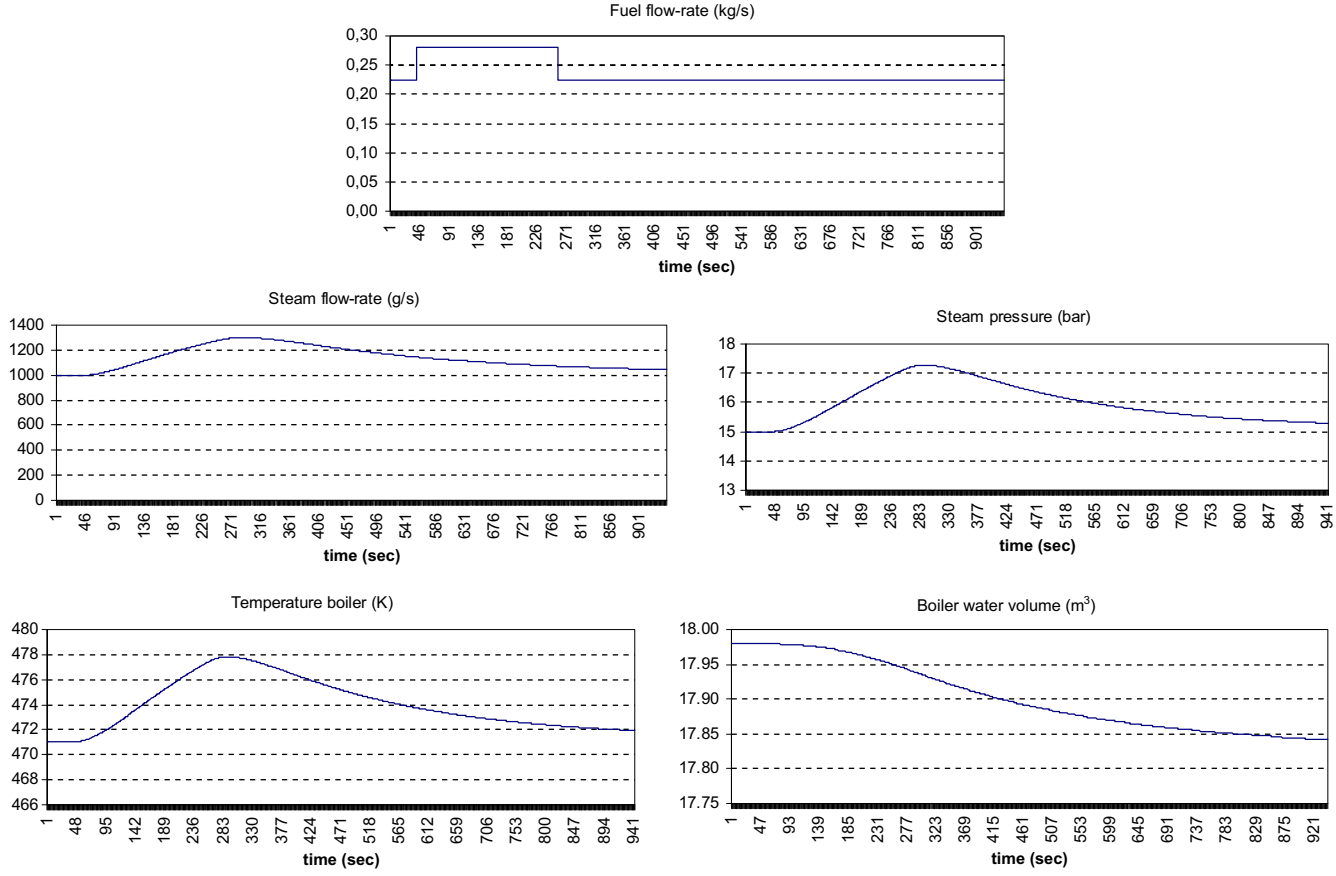

Fig. 7. Dynamic behavior of the boiler under a pulse in fuel flow-rate from 0.22 to 0.28 kg/s and back to 0.22 kg/s.

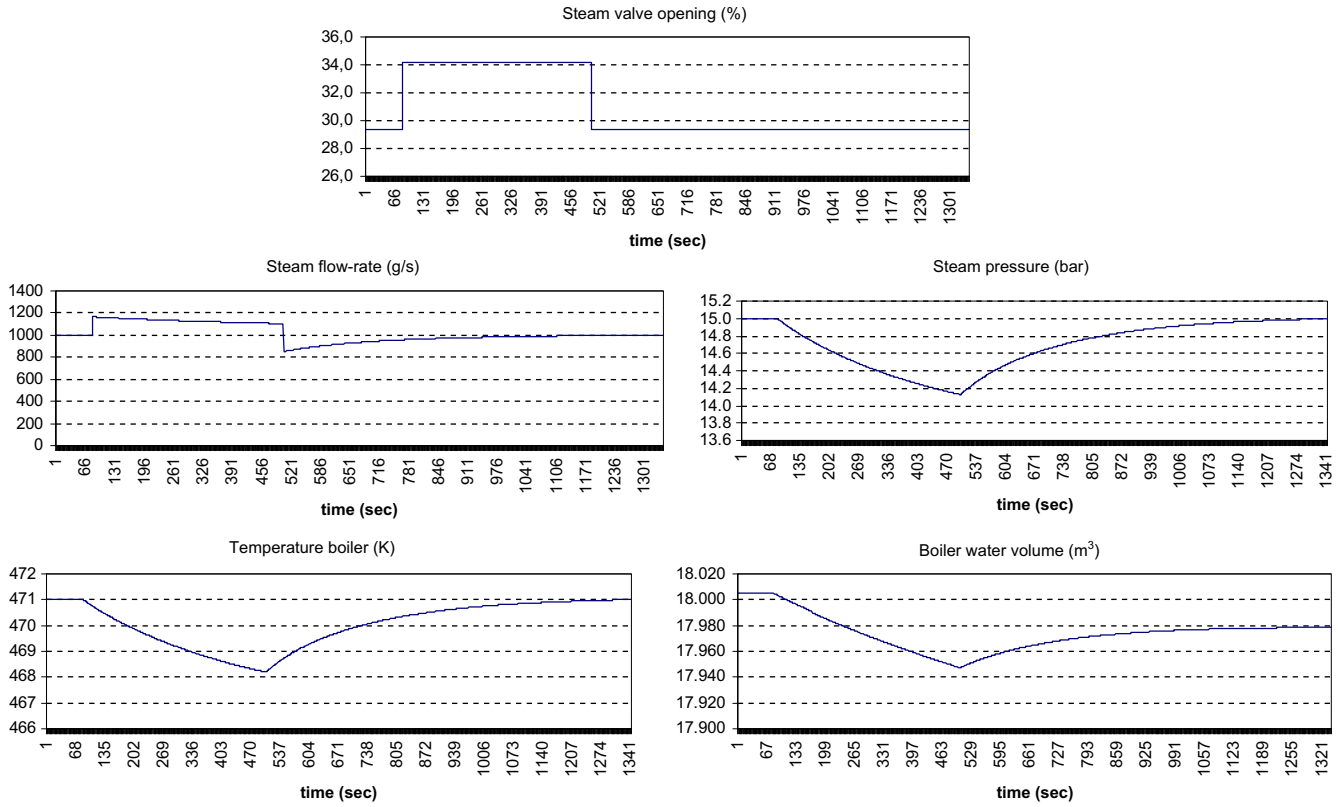

Fig. 8. Dynamic behavior of the boiler under a pulse in steam valve opening from 29.2 to 34.3% and back to 29.2%.

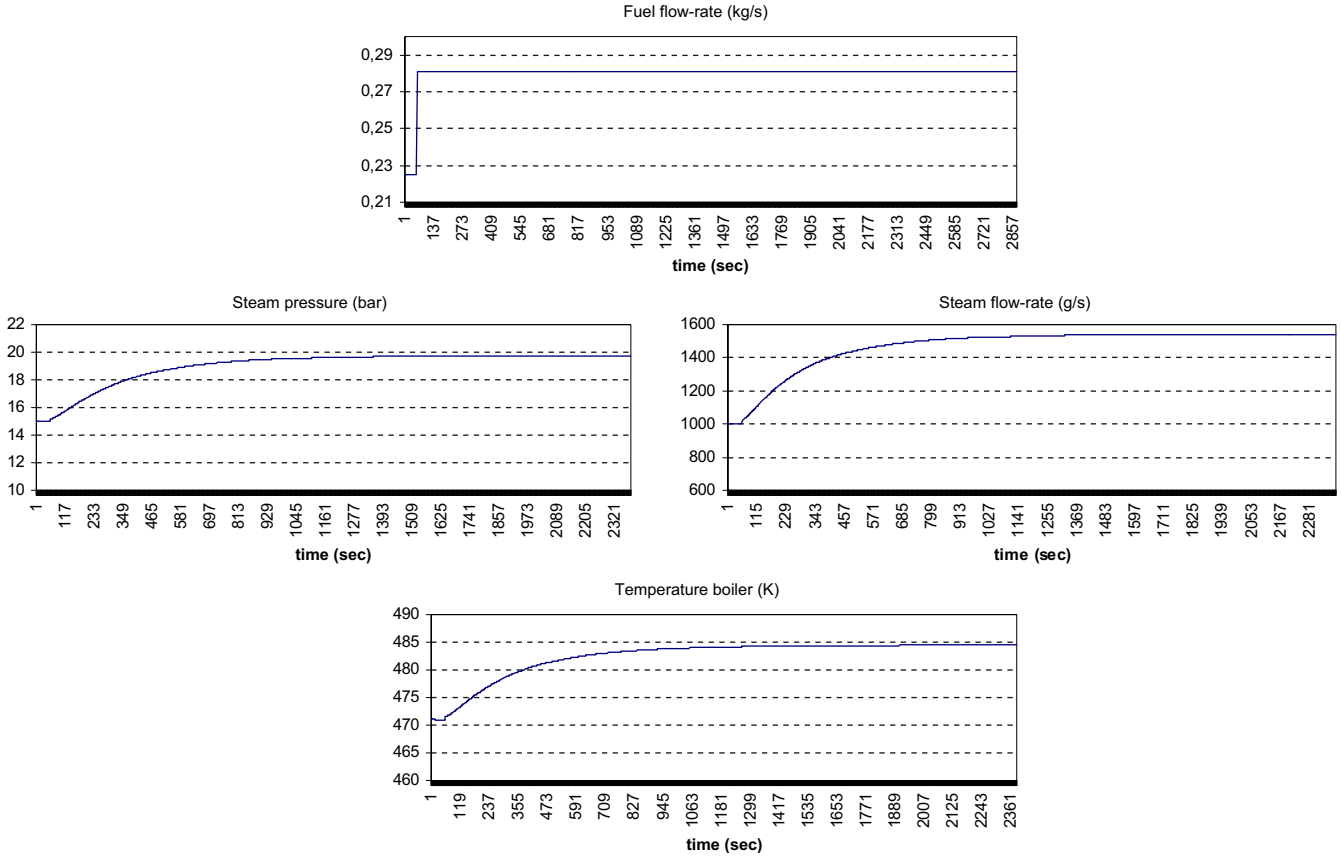

Fig. 9. Dynamic behavior of the boiler under a step in fuel flow-rate from 0.22 to 0.28 kg/s.

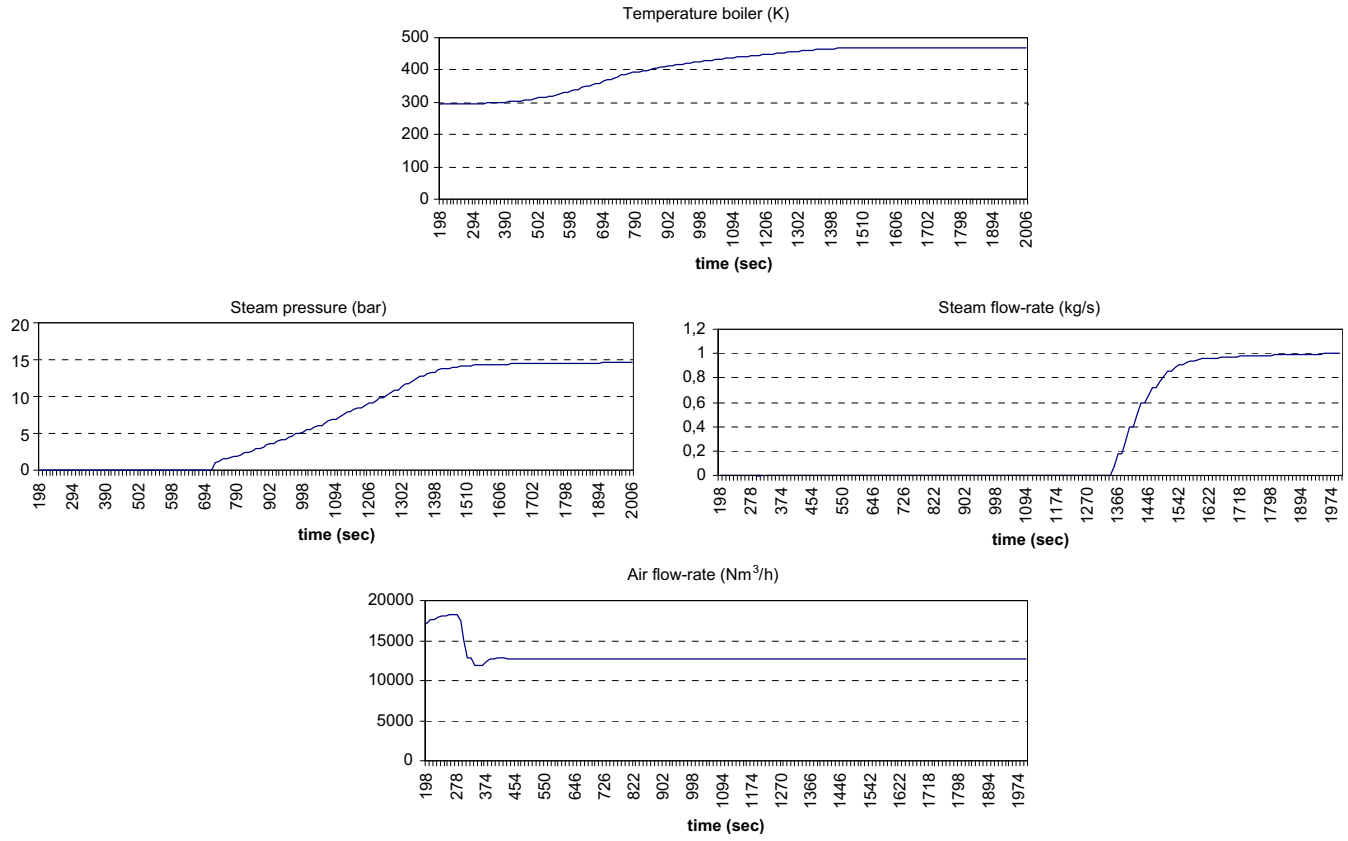

Fig. 10. Dynamic behavior of the boiler during the start-up initiated at $t = 0$.

blown with air, so the air flow-rate firstly increases when flame is established in boiler, for a fuel flow-rate of 0.22 kg/s, but then it always goes down progressively in order to get an oxygen concentration of about 4 %vol. The results for the start-up simulation are close to those shown by Krüger et al. [26].

6. Conclusions

A complete dynamic model of a full-scale fire-tube boiler has been developed based on the mass, energy, and momentum balances together with constitutional equations. Two parts are distinguished in fire-tube boilers: the fire/gas side and the water/steam side. A first nonlinear physical model has been presented and after reduced to shorten the computational time, but providing reasonable results. The boiler start-up has been also taken into account. Thus, it may allow to simulate the process as well as to design a multivariable controller. Simulation is useful both for training and assisting in on-line decisions. A case study has been simulated using an 800 HP fire-tube boiler and dynamic performances predicted by the model are in good qualitative agreement with data taken from the literature.

The proposed modeling may be used as an effective way of undertaking a comparison between the fire-tube boiler performances when running with different fuels, especially when considering the firing of a new fuel in given equipment. Another application may be the tests facilities used in research projects dealing with oxy-combustion process, since the model may be easily adapted to those operating conditions. Anyway, continued efforts are required to improve the model and to provide verification using more experimental data.

References

[1] O. Aydin, Y. Erhan Boke, An experimental study on carbon monoxide emission reduction at a fire tube water heater, Appl. Therm. Eng. 30 (2010) 2658–2662.
[2] A. Behbahani-nia, M. Bagheri, R. Bahrampoury, Optimization of fire tube heat recovery steam generators for cogeneration plants through genetic algorithm, Appl. Therm. Eng. 30 (2010) 2378–2385.
[3] P. Colonna, H. van Putten, Dynamic modeling of steam power cycles. Part I—modeling paradigm and validation, Appl. Therm. Eng. 27 (2007) 467–480.
[4] F.P. de Mello, Boiler models for system dynamic performance studies, IEEE Trans. Power Syst. 6 (1991) 66–74.
[5] E.J. Adam, L. Marchetti, Dynamic simulation of large boilers with natural recirculation, Comput. Chem. Eng. 23 (1999) 1031–1040.
[6] K.J. Astrom, R.D. Bell, Drum-boiler dynamics, Automatica 36 (2000) 363–378.
[7] H. Kim, S. Choi, A model on water level dynamics in natural circulation drum-type boilers, Int. Commun. Heat Mass 32 (2005) 786–796.
[8] P.J. Coelho, P.A. Novo, M.G. Carvalho, Modelling of a utility boiler using parallel computing, J. Super Comput. 13 (1999) 211–232.
[9] C.K. Westbrook, Y. Mizobuchi, T.J. Poinsot, P.J. Smith, J. Warnatz, Computational combustion, P. Combust. Inst. 30 (2005) 125–157.
[10] A. Gómez, N. Fueyo, L.I. Díez, Modelling and simulation of fluid flow and heat transfer in the convective zone of a power-generation boiler, Appl. Therm. Eng. 28 (2008) 532–546.
[11] M. Pezo, V.D. Stevanovic, Z. Stevanovic, A two-dimensional model of the kettle reboiler shell side thermal-hydraulics, Int. J. Heat Mass Tran. 49 (2006) 1214–1224.
[12] A. Habibi, B. Merci, G.J. Heynderickx, Impact of radiation models in CFD simulations of steam cracking furnaces, Comput. Chem. Eng. 31 (2007) 1389–1406.
[13] C.K. Weng, A. Ray, X. Dai, Modeling of power plant dynamics and uncertainties for robust control synthesis, Appl. Math. Model. 20 (1996) 501–512.
[14] M.E. Flynn, M.J. O'Malley, A drum boiler model for long term power system dynamic simulation, IEEE T. Power Syst. 14 (1999) 209–217.
[15] H.C. Hottel, A.F. Sarofim, Radiative Transfer. Mc-Graw-Hill, New York (USA), 1967.
[16] E. Talmor, Combustion Hot Spot Analysis for Fired Process Heaters. Gulf Publishing, Houston, TX (USA), 1982.
[17] M.G. Cooper, Heat flow rates in saturated nucleate pool boiling – A wide-ranging correlation using reduced properties, Adv. Heat Tran 16 (1984) 158–239.

[18] A. Chaibakhsh, A. Ghaffari, S.A.A. Moosavian, A simulated model for a once-through boiler by parameter adjustment based on genetic algorithms, Simul. Model. Pract. Th.15 (2007) 1029–1051.
[19] F.P. Incropera, D.P. DeWitt, Fundamentals of Heat and Mass Transfer, fifth ed. Wiley, NJ (USA), 2002.
[20] J.J. Wei, B. Yu, H.S. Wang, Heat transfer mechanisms in vapor mushroom region of saturated nucleate pool boiling, Int. J. Heat Fluid Fl 24 (2003) 210–222.
[21] Babcock-Wilcox, Steam: Its Generation and Use, 40th ed. The Babcock & Wilcox Company, New York (USA), 1992.
[22] B.J. Huang, P.Y. Ko, A system dynamics model of fire-tube shell boiler, J. Dyn. Syst-T ASME 116 (1994) 745–754.
[23] K. Sørensen, C.M.S. Karstensen, T. Condra, N. Houbak, Modelling and simulating fire tube boiler performance, in: Proceedings from SIMS 2003–44th Conference on Simulation and Modeling on September 18–19, Session 2b, Lecture 7, 2003 in Västerås, Sweden (ISBN 91-631-4716-5).
[24] C.M.S. Karstensen, K. Sørensen, Modelling of a one pass smoke tube boiler, in: Proceedings of SIMS 2004-45th Conference on Simulation and Modeling on September 23–24, 2004. 365–372. Copenhagen, Denmark (ISBN 87-7475-316 9).
[25] J.R. Rodriguez Vasquez, R. Rivas Perez, J. Sotomayor Moriano, J.R. Peran Gonzalez, System identification of steam pressure in a fire-tube boiler, Comput. Chem. Eng. 32 (2008) 2839–2848.
[26] K. Krüger, R. Franke, M. Rode, Optimization of boiler start-up using a nonlinear boiler model and hard constraints, Energy 29 (2004) 2239–2251.
[27] T.M.I. Mahlia, M.Z. Abdulmuin, T.M.I. Alamsyah, D. Mukhlishien, Dynamic modeling and simulation of a palm wastes boiler, Renew. Energy 28 (2003) 1235–1256.
[28] S. Lu, B.W. Hogg, Dynamic nonlinear modelling of power plant by physical principles and neural networks, Int. J. Elec. Power 22 (2000) 67–78.
[29] J.S. Truelove, Thermal and Hydraulic Design of Heat Exchangers, Furnace and Combustion Chamber, Heat Exchanger Design Handbook. Hemisphere Publishing Corporation, New York (USA), 1983.

Nomenclature

A: transfer surface (m^2)
$A/F)_t$: air/fuel stoichiometric ratio (kg/kg)
$A/F)_{real}$: air/fuel real ratio (kg/kg)
C: carbon content (weight fraction)
C_p: specific heat at constant pressure (kJ/(kg °C))
C_v: specific heat at constant volume (kJ/(kg °C))
CTM: global specific heat of the metal section (combustion chamber and tubes) (J/°C)
$\overline{e}$: average wall thickness of metal tube (m)
AE: air excess (fraction)
$f(x)$: inherent characteristic of the control valve (linear: $f(x) : x$)
fc: condensed water fraction recycled (fraction)
$RH(\%)$: relative humidity in the inlet air (%)
h: specific enthalpy (kJ/kg)
$\overline{h}_{c,water}$: average convective heat transfer coefficient of the liquid water (kJ/(m^2 °C s))
H_{burner}: energy supplied by the burner fan to balance the mechanical energy loss (m)
H_{fan}: energy supplied by the flue-gas fan to balance the mechanical energy loss (m)
$\overline{k}_t$: average thermal conductivity of the metal (kJ/(m °C s))
K_{VS}: flow coefficient of the control valve
LHV: lower heat value (MJ/kg: 10^3 kJ/kg)
l: boiler height (horizontal cylinder) (m)
L: boiler length (m)
m: mass (kg)
$\dot{m}_{air})_{t,dry}$: mass flow-rate of the theoretical dry air (kg/s)
$\dot{m}_{air})_{t,wet}$: mass flow-rate of the theoretical wet air (kg/s)
$\dot{m}_{fuel}$: mass flow-rate of the fuel (kg/s)
$\dot{m}_g$: mass flow-rate of the flue gas (kg/s)
M: molecular weight (kg/kmol)
$n_{t,j}$: number of tubes in the gas pass through a given tube bank, j
Pd: power losses (kW)
$P_V(T)$: vapor pressure at temperature T (bar)
P: pressure (bar)
$\dot{Q}_{g\to w}$: heat released to the water (kJ/s)
$\sum_j \dot{q}_{j,water}$: heat gained by water (kJ/s)
R_g: perfect gases constant (0.082 (atm l)/(mol K))
$R_{ext,H}$: exterior radius of a tube (m)
t: time (s)
T: temperature (°C)
V: volume (m^3)
v_g: gas velocity (m/s)
v: specific volume (m^3/kg)
x: fraction of valve opening (−)
x_v: vapor quality (kg vapor/kg total)
Y: variation of the fractional heat release due to combustion with axial distance (−)
z: geometric height (m), used in momentum balance

Greek
α: efficiency factor for heat flow losses due to convection and radiation
ϵ: emissivity
$\overline{\lambda}$: average latent heat of the water (kJ/kg)
η: fuel-steam efficiency
ρ: density (kg/m^3)

Subscripts:
H_2O: water
amb: ambient o atmospheric (around the boiler)
chim: chimney
cons: consumed in a chemical reaction
in: inlet
f: feed water
F: relative to combustion chamber or furnace
g: flue gas
gen: generated in a chemical reaction
j: number of the gas pass (through a given tube bank: 2, 3 or 4)
p: purge (water or air)
wall: tube wall
out: outlet
sum: downstream from the steam control valve (to the use points)
t: metal tube
total: relative to all the water/steam side (liquid and steam)
v: vapor or steam

Superscripts
i: slices in furnace and tubes
+: vapor/air phase inside the boiler (upper zone)
−: liquid phase inside the boiler (lower zone)